SYNTHESIS OF MOLYBDENUM BASED NANO COMPOSITES FOR DESULFURIZATION OF MODEL FUELS

BY

UMAR CHECHE ABUBAKAR

A Thesis Presented to the
DEANSHIP OF GRADUATE STUDIES

KING FAHD UNIVERSITY OF PETROLEUM & MINERALS

DHAHRAN, SAUDI ARABIA

In Partial Fulfillment of the
Requirements for the Degree of

MASTER OF SCIENCE

In

CHEMISTRY

MAY, 2017

KING FAHD UNIVERSITY OF PETROLEUM & MINERALS

DHAHRAN- 31261, SAUDI ARABIA

DEANSHIP OF GRADUATE STUDIES

This thesis, written by UMAR CHECHE ABUBAKAR under the direction of his thesis advisor and approved by his thesis committee, has been presented and accepted by the Dean of Graduate Studies, in partial fulfillment of the requirements for the degree of **MASTER OF SCIENCE IN CHEMISTRY.**

Dr. Tawfik Saleh
(Advisor)

11/12/2017

Dr. Abdulaziz Al-Saadi
Department Chairman

Dr. Khalid Alhooshani
(Member)

Prof. Salam A. Zummo
Dean of Graduate Studies

Dr. Jameel Al-Thagfi
(Member)

18/12/17

Date

DEDICATION

To my beloved family

ACKNOWLEDGMENTS

All praise belongs to Allah, The Lord of all that exist. Thanks to my advisor, Dr. Tawfik Saleh and members of my thesis committee; Dr. Khalid and Dr. Jameel Al-Thagfi. I appreciate the support of all the faculty and staff members of chemistry department especially Dr. Abdulazeez Al-Saadi, Dr. Bassam El Ali, and all those who have taught me. Specials thanks to the Nigerian community in KFUPM for their immeasurable support especially at crucial moments. I would like to express my profound gratitude to KFUPM and the Kingdom of Saudi Arabia for the scholarship opportunity.

I would like to acknowledge the sacrifice from my family, friends and all those that have ever supported me in any way. Special thanks to my parents and guardians for the uncommon love and benevolence. I am very grateful for the immeasurable support from my beloved wife and I would like to confess that I feel hugely indebted to her and adorable children, Abdullah and Rahma. I pray that Allah reward you all and make all the efforts beneficial.

TABLE OF CONTENTS

LIST OF TABLES

LIST OF FIGURES

LIST OF ABBREVIATIONS

AC	**:**	**Activated Carbon**
BET	**:**	**Brunauer-Emmett-Teller**
BT	**:**	**Benzothiophene**
CA	**:**	**Citric Acid**
CoMo	**:**	**Cobalt Molybdenum**
DBT	**:**	**Dibenzothiophene**
EDTA	**:**	**Ethylenediaminetetracetic Acid**
FT-IR	**:**	**Fourier Transformed Infra-red**
HDS	**:**	**Hydrodesulphurization**
MOFs	**:**	**Metal Organic Frameworks**
Mo	**:**	**Molybdenum**
Ni	**:**	**Nickel**
NiMo	**:**	**Nickel Molybdenum**
XRD	**:**	**X-ray Diffraction**
XPS	**:**	**X-ray Photo-electron Spectroscopy**

ABSTRACT

Full Name : Umar Cheche Abubakar

Thesis Title : Synthesis of Molybdenum Based Nano Composites for Desulfurization of Model Fuels

Major Field : Chemistry

Date of Degree : May, 2017

The aim of this proposal is to formulate a series of Mo based catalysts that will be used for hydrodesulphurization of models fuel oils. Desulfurization is significant in the refining process of crude oil because sulfur containing compounds cause environmental pollution, poison catalysts, and corrode refining equipment. There are ongoing efforts to lower the limits of sulfur in all kinds of oils and one of the major areas that have continued to attract tremendous attention is the fabrication of materials that act more effectively as adsorbent/catalyst compared to the existing ones that have been reported as viable alternatives to the existing materials for the desulfurization of fuels.

In this work, activated carbon produced from waste tires was used as a support for hydrodesulphurization catalysts, Ni and Mo. The prepared catalysts were then used for the desulfurization of dibenzothiophene in a batch reactor at a hydrogen pressure of 50 bar and temperature 350 ^{0}C. Results show an appreciable level desulfurization and further modifications were carried out to improve the activity of the catalysts. Thus, ultra-sonication and chelating agents were used to enhance the dispersion of the active phase on the support. The prepared catalysts were characterized by different techniques and instruments to establish the inherent properties of the materials. X-Ray diffraction (XRD),

X-ray photoelectron spectroscopy (XPS), Fourier transform IR (FT-IR) , scanning electron microscopy (SEM) and Brunauer–Emmett–Teller (BET) measurements were all utilized to explain the properties of the hydrodesulfurization catalyst.

A further modification was achieved by combining the activated carbon with TiO_2 through the sol-gel and hydrothermal synthesis. Enhanced performance was observed with catalysts supported on the carbon-TiO_2 composite under the same operations. In fact, the no trace DBT was found after 4 hours of reaction at 350^{o}C and hydrogen pressure of 50 bar.

The results of the study showed that activated carbon from waste tires and the activated carbon-metal oxide composite can be used as alternative support material for HDS catalysts to reduce the cost of refining crude oils and at the same time eliminate the negative impacts of waste disposal.

ملخص الرسالة

الاسم الكامل: عمر تشيش أبو بكر

عنوان الرسالة: تحضير مركبات الموليبدينيوم مدمجة مع الكربون لإزالة الكبريت من الوقود

التخصص: كيمياء

تاريخ الدرجة العلمية: مايو 2017

تهدف هذه الدراسة إلى تحضير سلسلة من المحفزات المكونة من الموليبدينوم نانوية الحجم مدعمة على أسطح من الكربون المحضر من الإطارات كمصدر رخيص التكلفة. إن إزالة الكبريت أثناء عملية تكرير النفط الخام هام جدا لأن المركبات المحتوية على الكبريت تسبب التلوث البيئي، والمواد الحفازة السامة، وتآكل معدات التكرير. وهناك جهود جارية لخفض حدود الكبريت في جميع أنواع الزيوت، وأحد المجالات الرئيسية التي واصلت اجتذاب اهتمام كبير هو تصنيع المواد الحفازة التي تعمل بشكل أكثر فعالية كبدائل قابلة للتطبيق مقارنة بالمواد الموجودة لإزالة الكبريت من الوقود.

في هذا العمل، تم استخدام الكربون المنشط الناتج من إطارات النفايات كداعم لمحفزات مكونة من المولبيدينيو والنيكل. ثم تم استخدام المحفزات المعدة لإزالة الكبريت من ثنائي البنزين ثيوفين في مفاعل عند ضغط هيدروجين 50 بار ودرجة حرارة 350 درجة مئوية. النتائج اظهرت إزالة الكبريت الى مستوى ملحوظ وأجريت المزيد من التعديلات لتحسين نشاط المحفزات. وهكذا تم استخدام الأسطح الداعمة المعدلة لتعزيز توزيع المواد الحفازة النانوية النشطة على الدعم.

وقد تم توصيف المحفزات المعدة بتقنيات وأدوات مختلفة لتحديد الخصائص المتأصلة للمواد. تم استخدام كل من التحليل الطيفي و حيود الأشعة السينية و التحليل الطيفي الضوئي بالأشعة السينية والفحص المجهري الإلكتروني لتحديد خصائص المركبات المحضرة.

تم إجراء تعديل آخر من خلال الجمع بين الكربون المنشط مع التيتانيا من خلال طريقة التحضير الكيميائى بالتسخين. وقد لوحظ تحسن في الأداء مع المحفزات المدعومة على مركب من ثاني أكسيد التيتانيوم والكربون تحت نفس العمليات مقارنة بالمحفزات المحضرة على سطح داعم من الكربون فقط.

وأظهرت نتائج الدراسة أن الكربون المنشط من إطارات النفايات مع التيتانيا دواعم جيدة لتوزيع الحفازات النانوية من الموليبدينوم وقد أوضحت النتائج فعالية جيدة للمواد الحفازة المحضرة في إزالة الكبريت من الوقود المحضر. المواد الحفازة المحضرة تتمتع بانها رخيصة التكلفة وبالتالي فإن استخدامها سيؤدي لتقليل تكلفة تكرير الزيوت الخام وفي الوقت نفسه القضاء على الآثار السلبية للتخلص من النفايات

CHAPTER 1

INTRODUCTION

1.1 Overview

Globally, crude oil is an invaluable source of energy and raw materials for major industries. However, the presence of sulfur compounds such as the thiophenes presents an enormous challenge in its utilization because these impurities lead to environmental pollution and increased the cost of refining due to catalysts poisoning, corrosion of refining equipment, and prevent the utility of fuel oils in applications such the fuel cells [1–3] .

1.2 Environmental Concerns

Compounds containing sulfur are found in most crude oil and other hydrocarbon fuels such coal and natural gas as impurities. The combustion of fuels containing sulfur species; especially the crude oil fractions such as gasoline, diesel and jet fuels; easily leads to the injection of SO_2 and fine particles into the environment [4]. The end result is environmental degradation, destruction of valuable properties and the spread of avoidable diseases. Thus, desulfurization is one issue of enormous significance in the refining process of crude oil as the demand for cleaner fuels increases. Coupled with the emerging stringent regulations due the environmental concerns around the globe makes the need to achieve complete desulfurization of fuels inevitable. For instance, Environmental Protection Agency (EPA)

regulations in the United States of America (USA) has limited the allowable sulfur concentrations to 30 ppmw and 15 ppmw for gasoline and highway diesel respectively[2].

1.3 Hydrodesulphurization (HDS)

Although HDS ensures the efficient removal of the light sulfur species such as the mercaptans, sulfides, and disulfides, some of the organosulfur compounds such as the thiophenes and the related derivatives are quite stable under conventional HDS conditions remain unaffected. HDS is ineffective for deep desulfurization because the aromatic sulfur compounds such as thiophene, benzothiophene (BT), and 4,6-dimethyldibenzothiophene (DMDBT) remain stable under the operating conditions. The efficient removal of these obstinate sulfur compounds to the desired levels require more severe conditions and sophisticated infrastructure[5]–[8]. Hence, facile alternative desulfurization methods under milder operation conditions are relentlessly being investigated.

Although each of the above-mentioned technologies has peculiar advantages, adsorptive desulfurization is considered a more viable potential alternative to HDS because operations can be done under ambient conditions. With the ideal adsorbent, high temperatures, high-pressure reactors, H_2 or corrosive reagents are required for desulfurization of through ADS. The basic requirements for the adsorbent in ADS method are: an excellent adsorptive capacity, peculiar adsorption selectivity towards the targeted sulfur compounds, stability, and ease of regeneration. Moreover, the materials are expected to be non-toxic, low cost and environment-friendly [9–12].

Extensive research has led to the successful fabrication and evaluation of several adsorbents and catalysts with different capacities for desulfurization. An ideal adsorbent

for desulfurization is expected to be cheap, porous, easily regenerated and exhibit excellent selectivity for the target compounds. Some of the materials that have been investigated include activated carbon, zeolite, TiO_2, Al_2O_3, silica, zirconia [13-14] as well as metal-organic frameworks (MOFs)[15] and porous organic polymers (POPs). Each of these adsorbent materials has unique properties and can be modified to enhance performance. These materials are often subjected to different treatment methods in order to increase the adsorptive capacity and selectivity towards the targeted sulfur compounds.

AC is one of the cheapest available materials being investigated. ACs have a characteristic large surface area and well developed internal pore structure desired in materials used as support for other active material in various applications especially HDS. The peculiar properties of AC allow for a higher degree of dispersion of the active catalysts[16–18]. Although several studies have been conducted on the utilization of different forms AC in HDS and ADS, there are few or no reports on the use of carbon derived from waste tires. Besides carbon in combinations with metal oxides as composite support for HDS catalysts are very few despite the promising potentials. Moreover, studies on the use of mixed metal oxide have shown enhanced activity for the supported HDS catalysts largely due to the increased surface area of the support and higher degree of dispersion of the active catalysts.

1.4 Statement of Problem:

Although adsorptive desulfurization has long been identified as a viable technique for the effective removal of refractory sulfur compounds from fuel oils under ambient conditions, the development of effective catalyst and ideal adsorbents with excellent adsorptive

capacity and selectivity towards the targeted sulfur compounds have continued to remain a challenge to researchers.

AC is one of the cheapest available materials being investigated. ACs have a characteristic large surface area and well developed internal pore structure desired in adsorbent materials and support for other active material in various applications especially ADS. The peculiar properties of AC allow for higher degree of dispersion of active the components such as metals and the metallic oxides.

Although several studies have been conducted on the utilization of different forms AC in ADS, reports on the use of bimetals or the combination of metals with metallic oxides on carbon support are few. Moreover, studies on photocatalytic degradation and the simultaneous adsorptive removal of the contaminants are mostly limited to the use of doped TiO2 zeolite supports.

1.5 Objectives:

This research work aimed to use metal nano particles formulate catalysts materials with exceptional capacity for the selective removal of the refractory organosulfur compounds found in fuel oils.

The specific objectives were:

- To prepare Mo catalysts supported on activated carbon (AC), TiO_2,and activated carbon/TiO_2 composite materials (ACT)

- To characterize the prepared materials using different techniques including IR, XRD, BET, TEM, SEM and EDX.
- To test the effectiveness of the supported catalysts in the HDS of DBT
- To investigate the role of calcination temperature and dispersion agents on the performance of the catalysts.

1.6 Significance of the Work

Major significance includes:

- Enhance fuel quality
- Reduce refining cost
- Environmental conservation and protection

CHAPTER 2

LITERATURE REVIEW

2.1 Desulfurization Techniques

Desulfurization is one of the key routine processes carried out in most crude oil refineries around the and the conventional hydrodesulfurization (HDS) technology is the most widely used. The process involves the use of a catalyst at high temperature (300–450^{0}C) and under high H_2 pressure (3–5 MPa) to yield hydrocarbon fuels containing a lower amount of Sulphur [19]. Thiophene (TP) and the related organosulfur compounds such as benzothiophenes (BT), methylbenzothiophenes (MBT) and dimethylbenzothiophenes (DMBT) are challenging contaminants found in crude oil. These aromatic contaminants are stable and therefore difficult to remove by the conventional means. The HDS technique ensures the removal of the non-aromatic and lower molar mass sulfur species while the refractory contaminants remain and are found often concentrated in the higher boiling fraction of the crude [20]. Consequently, further desulfurization is required before these fuels used in order to guarantee full utilization and safety.

A lot of resources have been deployed to come up with more viable alternatives to HDS for the effective removal of the refractory organosulfur compounds in hydrocarbon fuels. Some of the key innovations include: oxidative desulfurization (ODS); biodesulfurization (BDS)[21] and [22]; ionic liquids and catalytic desulfurization[23], [24] and [25]; and photocatalytic oxidative desulfurization (PODS)[26],[27] and [28]; and adsorptive desulfurization (ADS)[29], [10],[30],[31],[32].

Extractive desulfurization (EDS) involves thorough mixing of the fuels with suitable solvents (such as acetone, ethanol, polyethylene glycols and ionic liquids) and subsequent separation to extract the organosulfur species. Although the operations are usually carried out under ambient conditions without catalysts or hydrogen supply, the selective removal of the target sulfur compound by the solvents is a major setback [33]. Thus, the organosulfur compounds are often oxidized to enhance solubility.

Oxidative desulfurization (ODS) involves the oxidation of the organosulfur compounds using oxidants (such as acids, hydrogen peroxide, oxygen, ozone etc.) and then the subsequent separation of the resulting sulfoxides or sulfones through extraction with a suitable solvent. The sulfones are more polar and therefore, easier to remove through extraction compared to BT and the related compounds. The ODS technique requires the use of an oxidant and a catalyst for efficient chemical conversions. [34], [35] and[36] .

Biodesulfurization (BDS) involves the use of microorganisms that have the inherent capacity to transform/utilize the organosulfur compounds especially through metabolism. The BDS approach requires a microbial system with the potential to act on the broad range of organosulfur compounds found in crude oil fractions [37]. BDS operates under ambient and it has additional advantages of high selectivity and minimal waste generation. However, the biodegradation process is slow and getting the ideal biocatalyst remains a challenge [21] -[22].

Photocatalytic desulfurization involves the use photocatalysts such as TiO_2 to remove or degrade the unwanted sulfur species from the fuels and the environment [23], [24]. The photocatalysts are is often dispersed onto support materials to facilitate adsorption and

seamless interaction with the substrate. Some of the materials used to support TiO_2 include SBA-15 the ,[25] photocatalytic oxidative desulfurization (PODS) is one of the major techniques that have been explored by researchers and it often involves the use of oxidizing agents like H_2O_2 [26],[27].

The ADS processes are of two types: reactive and nonreactive ADS. The reactive adsorption (RADS) processes involve the use of adsorbents and high temperatures to remove the sulfur atom from the organosulfur compounds while the remaining hydrocarbon component is recovered. The sulfur is held on the sorbent and then later removed to regenerate the adsorbent for reuse. Several adsorbents have been formulated and investigated for used in the reactive adsorption desulfurization [38]. In fact, ConocoPhillips has already developed and commercialized the S-Zorb, a new process for the production of low-sulfur gasoline [39].

In the case of nonreactive adsorption, high temperatures are not required, and the organosulfur compounds are successfully removed by physisorption on the surface/matrix of the adsorbent material. Nonreactive ADS under ambient conditions is considered one of the most promising approaches to obtaining cleaner fuels and safer fuels[40]. Considering the fact, the desired goal can be achieved at a lower cost since all operations are expected to be carried out under ambient conditions without the use hydrogen or oxidants. Thus, tremendous effort has been devoted to the development of suitable adsorbents and the modification of existing ones to meet the required specifications.

2.2 Catalysts Supports and Adsorbents

Adsorption is one of the key separation tools well suited for purification applications and difficult separations. Extensive research has been done on the formulation of adsorbents with tailored porosities and surface chemistry for applications in various field including energy, gas storage, water treatment gas storage and separation [41]. The desire for cheaper, efficient and easily regenerated adsorbent materials possess high capacity for selectivity for the removal sulfur compounds is a key motivation for the current efforts in material development. Although some commercial adsorbents are available, cheaper and more efficient alternatives can be obtained from a variety of sources for the desired applications. including waste[42],[43]. Several adsorbents of various components have been formulated and tested and tested particularly for the liquid phase desulfurization of hydrocarbon fuels. Examples include carbon, zeolites, alumina, zirconia, MOF, POPs and their derivatives.

2.2.1 Carbon Supports

Activated carbon is one of the most popular and widely used adsorbents throughout the world. It is derived from a variety of cheap carbon-based materials such as wood, coal, lignite, coconut shell and even wastes rubber tires. Activated carbons (AC) prepared from various sources have been utilized as adsorbents especially in water and wastewater treatment as well as in the ADS of fuels[44]. For example, AC can be easily obtained from waste such as coconut coir[45], waste tires[46],[9] , and sewer sludge[47].

ACs has a characteristic large surface area and well developed internal pore structure consisting of micropores, mesopores, and macropores. The inherent properties such as surface area and porosities of ACs are, to a large extent, influenced by the parent materials

and the method employed in their production. Surface modification of activated carbons by different treatment methods has been investigated. Some of the modification methods had been reported include treatment with acids and bases, impregnation or loading with metals, oxidation with ozone, as well surface treatments with plasma and microwaves. All of these methods have been used to enhance the adsorption performance of the adsorbent materials by increasing the number active adsorption sites on the surface. For instance, the surface properties of AC is often modified by suitable thermal or chemical treatments to improve to improve its adsorption capacity and selectivity towards targeted contaminants, [48], [49],[44].

Reports on the influence of treatment conditions indicate that the adsorptive capability of AC was improved significantly on treatment with acids[9], [47]. It has been established the adsorption capacities, adsorption selectivity and rates of adsorption are directly linked to surface area and pore size distribution of the adsorbent. Acids such as HNO_3, H_2SO_4, and HNO_3/H_2SO_4 solutions can be used to form acidic groups on the carbon surface. These acidic groups can interact with the hetero atoms in thiol and thiophenes through intermolecular hydrogen bonding to enhance adsorption to the carbon surface. Thus, the selective adsorption of molecules is governed by the amount of oxygen-containing complexes which are predominantly created on the surface of AC through oxidation [50].

Several studies had been conducted on modification AC through impregnation with metals, especially the transition metals that act as active sites. The results indicate that the adsorption capacity and selectivity of the impregnated AC changes, depending on the type and amount of metal as well as the preparation conditions. [51], [52], [53] . Metals such as Ag, Ni, Cu, Al, Fe Mn and several others have all been loaded on AC for utilization in

adsorptive desulfurization. For example, while Ni catalysts supported on acid-treated ACs were used for the adsorptive removal of SO_2 from flue gas, Mn-based AC catalysts were successfully used for desulfurization similar studies [54]. Modulation of adsorption capacity towards various organosulfur compounds was observed on impregnation of AC with $CuCl_2$ in a study of the deep desulfurization of fuel gas [55]. Acid-treated AC impregnated with $PdCl_2$ showed enhanced adsorption efficiency for the desulfurization of diesel when compared to the performance of the parent AC material [47]. Recently, Thaligari et al. demonstrated that nickel-modified granular activated carbon could be used for the simultaneous desulfurization and denitrogenation of liquid fuels [56]. The observed enhancement in adsorption capacity of AC, when impregnated with transition metal chlorides, is attributed to the resulting increase in the number of adsorption sites on the carbon surface[57].

Metal species with π-complexation capabilities where observed to have significantly higher adsorption capacities for sulfur[1]. For example, the $PdCl_2$/AC was observed to have a higher adsorption capacity than both Pd/AC and CuCl/AC tested under the same conditions. The observed trend was attributed to the fact that Pd^{2+} has a stronger tendency for π-complexation. Further investigations also revealed that AC is a more effective support for π-complexation reagents than Al_2O_3 and even zeolite. In addition, a remarkably higher adsorption selectivity was observed for $PdCl_2$/AC compared to the pristine AC [58].

Recent studies have shown that AC could be loaded with more than one active components at a time to form more effective adsorbents/catalyst. For instance, it was demonstrated that Fe/Mo/AC composite could be used for the effective removal of both H_2S and carbonyl sulfide (COS) from coal gas. The adsorption capacity of the ZnO/AC composite for H_2S

was found to improve on the partial substitution of the ZnO with CuO on the AC support to form the bimetallic composite CuO/ZnO/AC [59]. AC obtained from waste rubber tires was loaded with both Ce and Fe to form the bimetallic composite, AC/Ce/Fe. The AC/Fe/Ce composite and composites of the individual metals, AC/Fe and AC/Ce, were all evaluated for the adsorptive removal of TP, BT and DBT in a hexane/toluene solvent under same conditions. The results showed a significant improvement in adsorption performance for all the composites but that the bimetallic composite exhibit the highest adsorption capacity compared to both AC/Ce and AC/Fe while all the adsorbents performed best towards the DBT compared to the other thiophenes. The bimetallic composite adsorbents also prove to be thermally regenerable and could, therefore, be used for several cycles in desulfurization [60].

It has been observed that loading AC with metals is accompanied by a change the porosity of the support, depending on the amount of the metals. [60]. A study on the effect of solvent polarity in the liquid phase adsorption of thiophene and other aromatic contaminants over MI-101 and AC was investigated and the results show that the AC was more effective in more polar solvents [61].

2.2.2 Zeolites

Zeolites are one of the most popular and extensively used materials especially in the petroleum industry throughout the world. The unique properties such the pore structures, large specific surface areas, thermal stability have made zeolites choice materials in applications such as catalysis and separation[62]. Substantial literature exists on the utilization of zeolites as adsorbents in the various application including HDS as well as ADS of fuels. Reports indicate that the cation-exchanged such as Cu(I)Y and Ni(II)Y are

effective in the removal of the sulfur compounds found in fuel oils. A study of as set of cation exchanged Y-zeolites (Ce(IV)Y Cu(II)Y, Ni(II)Y, Zn(II)Y and Pd(II)Y) revealed that Ce(IV)Y has the highest adsorption selectivity when compared with the others [63]. Meanwhile, a clinoptilolite zeolite was recently reported to exhibit more favorable adsorption isotherm for thiophene, BT, DBT as well as isopropyl mercaptan (IPM) (upon dealumination and further ion-exchange with Ni^{2+} [64].

It has been observed that Ag(I) and Cu(I) containing sorbents used to have exceptionally higher adsorption capacities and adsorption selectivities compared to the other transition metal due to their π-complexation capabilities. [1]. For example, the Cu(I)Y sorbent was found to be a superior adsorbent in terms of adsorption capacity and selectivity compared to the other adsorbents used under the same conditions[65]. The observed trend was attributed to the fact that Pd^{2+} has a stronger tendency for π-complexation than Cu^{+} and Pd^{0}. Further investigations also indicate that AC is a more effective support for π-complexation sorbents than Al_2O_3 and even zeolite. In addition, a remarkably higher adsorption selectivity was observed for $PdCl_2$/AC compared to the pristine AC [58].

A study on the impacts of substrates on π-complexation showed that the silica was a more amenable substrate for the adsorption of olefin on monolayer $AgNO_3$ compared to both MCM-14 and γ-Al_2O_3. The observed phenomena were attributed to the lack of Lewis acid sites unlike in the case γ-Al_2O_3.Thus, the Ag atoms supported on SiO_2 are more likely to form π-complexation bonds with the olefins.

In recent times, researchers have resorted to the combination of two different metals to obtain bimetal ion exchange zeolites. For example, the Cu- Ce bimetal ion-exchanged Y-

zeolite Cu(l)-Ce(lV)-Y, was fabricated and used for ADS. The new material exhibited the highest adsorption capacity and selectivity for the thiophenic compounds when compared to both Cu-Y and Ce-Y. The enhanced performance was attributed to the synergistic interaction between Cu^{2+} and Ce^{4+} since Cu-y was observed to have a high adsorption capacity but low adsorption selectivity while Ce-Y has low adsorption capacity but high adsorption selectivity for the thiophenes [66]. Similarly, Ni and Ce loaded Y zeolite, Ni-Ce-Y, was observed to have higher adsorptive selectivity for DBT in a model than Na-Y, Ni-Y, and Ce-Y [29]. The bimetallic Ag-Ce-Y was also exhibited high adsorptive capacity and high adsorption selectivity to organic sulfur compounds in model fuels containing toluene or cyclohexene [30], [32].

2.2.3 Metal Organic Frameworks

Metal organic frameworks (MOFs) are a diverse set of crystalline materials with highly porous structures [67]. These crystalline materials are constructed by various combinations of metal ions and organic ligands using any of the viable strategies which include hydrothermal and solvothermal synthesis [68] and [69]. Prominent examples include MOF-5, HKUST-1, MIL-100, MIL-101 etc. The properties of MOFS such as surface area and porosity can be effectively controlled by selection of the appropriate building blocks and there are various techniques that allow the incorporation of desired functionalities into the framework [70]. Techniques such as the post-synthetic modification (PSM), solvent-assisted linker exchange (SALE), and defect engineering (DE) have been effectively used to tailor MOFs for the desired applications[71], [72] and [73]. Thus, MOFs have become popular, particularly in areas of applications such as gas storage and separation, catalysis,

magnetism, electrochromism and chemical sensing as well as liquid phase separation [74], [75].

Recently, the applications of MOFs have been extended to utilization as adsorbents in liquid phase separations especially ADS and AND. in the quest for cleaner and affordable fuels. MOF-505, HKUST-1, UMCM-150, [76], MIL-100-Fe [77], MIL-100-Cr [15] have all been tested for the adsorptive removal of the various organosulfur found in fuels. Cychosz et al. reported that MOF-5, HKUST-1, and UMCM-150 have higher adsorption capacity than zeolite (NaY). In fact, MIL-47 was observed to have a superior adsorption capacity for BT compared both MIL-43(Al) and MIL-43(Cr), and only slightly less than the ion-exchanged CuY [78]. In general, MOFs with coordinatively unsaturated Cu-metal sites, UMCM-150 and MOF-505, were observed to have the highest adsorption capacity [75].

In terms of adsorption selectivity, UMCM-150, and MOF-505 A study on the adsorption selectivity performance of MOFs and zeolites indicate that HKUST-1 can selectively adsorb thiophene from a mixture containing toluene, while NaY showed no significant selectivity.

MOFs are now considered highly promising adsorbent materials for the adsorptive desulfurization fuels and other adsorption applications[12]. Factors affecting the adsorption capacity of a series MOFs were examined in a bid to correlate their properties (e.g., surface area, window diameter, and metal site) and performance. The results indicate that the metal structures of MOFs and the metal sites in the frameworks are the main factors are responsible for the different adsorbate−adsorbent interactions which in turn plays a

significant role in adsorptive desulfurization. While the interactions of the metal sites in MOFs with the with the delocalized π electrons of the aromatic rings aromatic of the sulfur compounds can be interpreted using Pearson's concept of hard and soft acids and bases (HSAB), selectivity is determined by the window diameter. Thus the performance depends on the type of metal sites and the size of the target contaminant[79].

The post-synthetic modification of MOFs allows the tailoring of these materials to the desired application. The new adsorbent proved to more stable compared to the previously reported IL-incorporated MIL-101s using different approach [80]. The incorporation of scandium-triflate ($Sc(OTf)_3$) onto MIL-101, UiO-66, and HKUST-1 resulted in a remarkable improvement in the adsorption capacity for both sulfur and nitrogen compounds compared to the pristine materials[31]. In a more recent report, vapor-induced selective reduction (VISR) technique was used to convert the Cu(II) sites in HKUST to Cu(I) in order to improve the performance in adsorptive desulfurization[81]. The ship-in-bottle (SIB) technique was used to incorporate ionic liquids (ILs) inside MIL-101 which was used for the liquid phase adsorption of BT from liquid fuel [82].

The effect of solvent polarity in the liquid phase adsorption of thiophene and other aromatic contaminants over MI-101 and AC was recently investigated and The results indicate that MOFs can be more effectively used in non-aqueous phase ADS as well as AND [61].

In contrast to zeolites and ACs, MOFs are not very stable at high temperatures. Therefore, the application is limited to mild conditions [12]. However, MOFs offer several advantages which include variety, vast topology and facile tenability [83].

2.2.4 Polymeric Supports

Polymer materials, especially the POPs are being explored as adsorbents in different areas of application in including: water treatment, gas storage, and separation, catalysis etc. POPs are advanced porous materials with remarkable features such as excellent stability and high surface area, well-defined porosity and choice functionalities[84] and [85]. Thus, their applications have been recently extended to ADS of fuels. It was recently demonstrated that POPs could be used as adsorbents for the effective removal of the organosulfur compounds often found in fuel oils. A triptycene-derived task-specific porous organic polymer (TSPOP) was tested for the adsorptive removal of BT. Compared to the popular and more widely used adsorbents such as AC and zeolites, the TSPOP showed modest a capacity for the adsorption BT from a model fuel, and loading the polymer material with Ag led to a remarkable enhancement in performance. The observed DBT capture capability of the adsorbent was attributed to π-π stacking between DBT and phenyl rings in the polymer matrix, while the enhanced performance on loading with Ag was a result of the additional π-complexation adsorption with Ag(I) ions. [86].

2.2.5 Metal Oxide Supports

TiO_2, Al_2O_3, and silica SiO_2 are some the prominent materials reported to have been used as adsorbents for the deep desulfurization of fuels. These metal oxides are often modified with transition metals known to act as an active site in order to increase their adsorption capacities for the various sulfur contaminants.

Metals Supported on different materials have been utilized as adsorbents and catalysts in various studies. For instance, silver oxide supported on TiO_2, Al_2O_3 and SiO_2 also showed notable improvements in adsorption capacity depending on the extent of dispersion of the silver oxide on the various supports[7]. TiO_2 has a lower surface area when compared to both Al_2O_3 and SiO_2. However, the surface area is increased if TiO_2 is dispersed on higher surface area supports. Thus, loading the mixed oxides TiO_2–Al_2O_3 and TiO_2–SiO_2 with Ag yielded effective adsorbents for the removal thiophene from fuel oils [5]. Recently, UV-assisted adsorption of BT over TiO_2 and Ag/ TiO_2 adsorbents were investigated. The results indicate an increased adsorption capacities for both adsorbents especially in the presence of H_2O additive in the model fuel [87]. In another related development, air-promoted ADS of low-sulfur diesel fuel over Ti-Ce mixed metal oxide, $Ti_{0.9}Ce_{0.1}O_2$, reported having a higher adsorption capacity compared to the individual metal oxides [88].

Besides the inherent susceptibility to the adsorption of sulfur compounds, some of the metal oxides, especially TiO_2, have been reported to exhibit photocatalytic activities that facilitate the desulfurization process. Although TiO_2 absorbs in the UV region of the electromagnetic region, doping with metals, carbon, nitrogen, and other elements extend the light absorption zone and enhance their photocatalytic efficacy under visible light [89]. For example, La/PEG/TiO_2 [90] and C/TiO2@MCM-41 [91] were reported to be effective in the photocatalytic degradation of DBT under visible light. WO_3. TiO_2, ZrO_2, and NiO jointly supported on ZSM-5 zeolite were reported to be effective in the photocatalytic oxidation desulfurization coupled with in-situ hydrogenation of gasoline. While H_2O_2 was used as the oxidant, mercury lamps were used as a light source [92].

2.2.6 Composite Support Materials

Composites support materials for catalysts are made by doping one of one material with the calculated amount of another to achieve a particular texture, morphology and other desired properties. Popular support materials such as carbon, TiO_2, Al_2O_3, and SiO_2 have been used in combination with different heteroatoms to formulate composite supports for catalysts used in various applications Important examples include dual metal oxides such as TiO_2-Al_2O_3, ZrO_2-Al_2O_3 and SiO_2-Al_2O_3 TiO_2, TiO_2-SiO_2 and several other combinations [93]. Other composite support formulations include carbon/metal oxides, polymer/CNT and those involving doping of carbon materials with heteroatoms such as nitrogen [94].

The composite materials are often designed to enhance stability and to facilitate dispersion of the active phase in order to achieve a higher activity of the catalysts. In some cases, the base materials are modified to introduce functionalities that will promote selectivity in order to achieve higher conversions of a substrate to a most preferred and specific product [95], [96] and [97].

The HDS activity of various metal catalysts supported on composite materials has been investigated. Recent works include the evaluation of synthesis techniques and their impacts on the properties of the synthesized composite materials. For example, HDS catalysts supported on supported on either TiO_2 or SBA-15 were found to be less effective compared to the same catalysts supported on TiO_2-SBA-15 composite made by the integration of the two support materials. Similar trends have been observed in with catalysts supported on mixed support materials used in HDS [98] and several other applications [93].

Some of the important reported works are listed in the following table as:

References	**Findings**	**Shortcomings**
Hu *et al.*, 2003	Carbon from waste tires was effective for adsorptive removal of thiophenes	Technique limited to fuels with low sulfur concentrations
Song *et al*., 2010	Impact of the sequence of impregnation on catalyst performance	Carbon obtained from a non sustainable source.
Hamdez *et a*l., 2014	negligible impact on the performance of supported catalysts	Involves complicated material procedures
Farag, Mochida and Sakanishi, 2000.	Discovered that CoMo was effective when supported on carbon than on alumina	The role of calcination temperature was not investigated.
Saleh and Danmaliki, 2016.	Carbon from waste tires was successfully used for the adsorptive removal of thiophene, BT, DBT and DMBT	Technique limited to fuels with low sulfur concentrations

Hu et al., 2016	N-doped mesoporous carbon was successfully synthesized and used as catalyst support	Valuable precursors were used and the catalyst was successfully tested only for the desulfurization of thiophene

CHAPTER 3

EXPERIMENTAL

3.1 Materials

Activated carbon (AC) derived from waste tires, ammonium molybdate [$(NH_4)_6Mo_7O_{24}.4H_2O$], nickel acetate [$Ni(C_2H_3O_2)_2.4H_2O$], cobalt nitrate [$Co(NO_3)_2.6H_2O$], decahydronaphthalene (decalin) [$C_{10}H_{18}$], dibenzothiophene (DBT) [$C_{12}H_8S$], citric acid (CA) [$C_6H_{10}O_7$], ethylenediaminetetracetic acid (EDTA) [$C_{10}H_{16}N_2O_8$], and deionized water [H_2O].

The ammonium molybdate, nickel acetate, and cobalt nitrate were A.C.S certified analytical grades from Fisher Scientific Company, USA. Decalin (99%) and DBT (98%) were obtained from Sigma Aldrich. All the reagents were used as purchased from the manufacturers without any form of pretreatment or modification.

3.2 Preparation of Support Materials

3.2.1 Preparation of activated carbon support

Activated carbon support was prepared from waste rubber tires according to the detailed procedure described in a previous report [99].

3.2.2 Preparation of TiO_2 Support

TiO_2 was prepared through a modified sol-gel and hydrothermal synthesis route reported in the literature. A dilute aqueous solution of $TiCl_4$ was prepared by adding 20 ml of $TiCl_4$ to 40 ml ethanol kept in an ice bath. The calculated amount of deionized water was added to the solution to form a 2 molar stock of $TiCl_4$. Appropriate amounts of the solution were taken in round bottom flask and then placed in an oil bath sitting on a hot plate/magnetic

stirrer. Drops of diluted aqueous ammonia were added to the solutions until a gel was formed while stirring at a solution was stirred at 350 rpm and the temperature was set at 80^0C. The gel was allowed to age for 24h before filtration and washing with distilled water to remove the excess base. The material was filtered an allowed to dry in an oven.

3.2.3 Preparation of Carbon-TiO2 composite support

6g of activated carbon was added to 80 ml of deionized water and stirred for 1 h. The mixture was transferred to a round bottom flask containing 20 ml of the $TiCl_4$ previously prepared. Then Drops of diluted aqueous ammonia was added to the solutions until a gel was formed while stirring at a solution was stirred at 350 rpm and the temperature was set at 80^0C. The gel was allowed to age for 24h before filtration and washing with distilled water to remove the excess base. The material was filtered an allowed to dry in an oven.

3.3 Preparation of HDS Catalysts

3.3.1 NiMo/AC, NiMo/TiO_2, and NiMo/AC-TiO_2

NiMo/AC was prepared through the co-impregnation of the activated carbon with Ni and Mo using aqueous solutions containing the appropriate amounts of their metallic salts. 6g of the activated carbon was added to aqueous solutions containing calculated amounts of the metal salts and subjected to continuous for 2hrs. Nickel acetate and ammonium heptamolybdate were used as the precursors to prepare a set materials containing 13wt. % Mo with the atomic ratios Ni/Mo maintained at 0.23 for all samples. Afterwards, the stirring was stopped and the solution allowed to evaporate at 70^0C and then dried at120^0 C for 24h. Both NiMo/TiO_2 and NiMo/AC-TiO_2 were prepared in exactly the same way as NiMo/Ac but $TiO_2$and AC-TiO_2 were used as support respectively. The dried materials were subjected to further calcination at 300 ^{o}C for 3hrs and then labeled accordingly.

3.3.2 Mo/AC, NiMo/AC and CoMo/AC

Mo/AC was prepared through the impregnation of the activated carbon with Mo using an aqueous solution of the salt containing 13 wt.% of the metal. NiMo/AC and CoMo/AC were prepared through the co-impregnation of the activated carbon with Mo and Ni or Co as indicated by the labels. the atomic ratios, Ni/Mo and Co/Mo, were 0.23 for both NiMo/AC and CoMo/AC while the total metal loading was maintained at 13 wt.%. at Mo using aqueous solutions containing the appropriate amounts of their metallic salts. In all cases, 6g of the activated carbon was added to aqueous solutions containing calculated amounts of the metal salts and subjected to continuous for 2hrs. Afterwards, the stirring was stopped and the solution allowed to evaporate at 70^0C and then dried at120^0 C for 24h. Some of the dried materials were subjected to further calcination at 300^{o}C for 3hrs and then labeled according to the materials' composition.

3.3.3 NiMo/AC, NiMo/AC 200, NiMo/AC300 and NiMo/AC400

NiMo/AC was prepared through the co-impregnation of activated carbon support with Ni and Mo as using aqueous solutions containing the appropriate amounts of their metal salts. 6g of the activated carbon was added to aqueous solutions containing calculated amounts of the metal salts and subjected to continuous for 2hrs prior to evaporation at 70^{o}C and the subsequent drying at 110^{o}C. NiMo/AC 200, NiMo/AC300 and NiMo/AC400 were prepared in the way as NiMo/AC but the catalysts were subjected to calcination for 3h at different temperatures after the drying at 110^{o}C. NiMo/AC 200, NiMo/AC300 and NiMo/AC400 were calcined at 200^{o}C, 300^{o}C and 400^{o}C respectively. The catalysts were labeled such that the figures reflect the calcination temperature and the composition of the prepared catalysts.

3.3.4 NiMo/AC, NiMo/AC(US), NiMo/AC(CA) NiMo/AC(EDTA)

NiMo/AC was prepared through the co-impregnation of activated carbon support with Ni and Mo as using aqueous solutions containing the appropriate amounts of their metal salts. 6g of the activated carbon was added to aqueous solutions containing calculated amounts of the metal salts and subjected to continuous for 2hrs prior to evaporation at 70^{o}C and the subsequent drying at 110^{o}C. As for NiMo/AC(US) 30 min. ultrasonication was used to facilitate the dispersion of the active metals during the impregnation. In the case of NiMo/AC(CA) and NiMo/AC(EDTA), chelating agents, citric acid and ethylenediaminetetracetic acid (EDTA), were used facilitate the dispersion of the active phase. In all cases, 6g of the support was used and the metal loading was maintained at 13wt.%. The impregnation mixture was allowed to evaporate at 70^{0}C and then dried at 120^{0} C for 24 h. The dried materials were subjected to calcination at 300^{o}C for 3h and then labeled using the initials of the to the dispersion medium.

3.4 Characterization of Support Materials and Catalysts

3.4.1 TGA

Dried catalysts without calcination were used for the TGA analysis and all experiments were conducted using a Mettler-Toledo TGA/SDTA 851^{e}, under static air atmosphere and a heating rate of 10 ◦C/min from 40 to 1000 ◦C

3.4.2 FT-IR

Fourier transform infrared spectroscopy (FT-IR) was used to identify the various functional groups present on the bare support and the catalysts supported on the carbon support using a Nicolet 6700 spectrometer (Thermo Electron). Pellets of the samples were made by adding KBr as a binder and then the absorption spectra obtained 64 scans.

3.4.3 XRD

Powder X-ray diffraction (XRD) of the passivated sample was performed on a Bruker D8 focus diffractometer, with Cu Kα radiation at 40 kV and 40 mA. Powder diffractograms were recorded at 12 $^{0}min^{-1}$ scanning speed over a 2θ range of 10–80^{0}.

3.4.4 Textural properties

N_2 adsorption–desorption isotherms were obtained for the bare activated carbon and then the supported catalysts after calcination at 300^{0}C under N_2 temperature. BET surface areas, pore volumes, and pore size distributions were measured under a liquid nitrogen atmosphere (−196^{0}C) using a micromeritics ASAP 2020 automatic analyzer. All samples degassed at 150^{0}C for 3h and then allow to cool before the experiments.

3.4.5 SEM -EDX

Scanning Electron Microscope JEOL – JSM6610LV was used to examine the morphology of the samples using secondary electron (SE) and backscattered electron (BSE) mode at an accelerating voltage of 20 kV, and the attached energy dispersive X-ray spectrometer (EDS, Oxford Inc.) detector was employed for subsequent elemental composition analysis and mapping of the elements in the samples.

3.5 Catalysts Activity Tests

The activity of the prepared catalysts towards the HDS of DBT was evaluated in a high-pressure batch reactor (model: Parr 4576B) at 350 °C under 5 MPa of H_2 pressure and constant 300 rpm stirring. 0.3 g of each catalyst was for reactions conducted using 100 ml of DBT fuel model. Decalin (decahydronaphthalene) was used as a solvent for the preparation of the model fuel containing 1000 ppm S (0.588g DBT). The activity tests lasted for 4 h after the reactor temperature reaches the set point of 350 ^oC and aliquots of the product were taken from the reactor at intervals of one hour. Prior to the tests, each of the catalysts was presulfided using a solution containing 2 wt.% CS_2 in a quartz tube at 350 °C for 5h after reduction with of 5% H_2/He (60 ml/min) at 400 °C for 2 h.

CHAPTER 4

RESULTS AND DISCUSSIONS

4.1 Characterization Results

4.1.1 Textural Properties of Support Materials and Catalysts

Textural properties of the support materials are presented in Table 1. Analysis of the results shows that AC has the largest BET surface area 583 m^2/g compared to 354 m^2/g and 310 m^2/g recorded for TiO_2 and AC-TiO_2 respectively. A similar trend is observed for the external surface area and micropore area of the three support materials. Although TiO_2 has a larger BET surface area and external surface area than AC-TiO_2, is important to note that the micropore area of TiO_2 is exceptionally small when compared to the micropore areas of AC and even AC-TiO_2 which is a composite of AC and TiO_2. The observations above indicate that AC, TiO_2, and AC-TiO_2 have unique surface and textural properties. Moreover, the total pore volumes, as well as the average pore diameter of the three support materials, are also different. While the total pore volumes recorded for AC, TiO_2 and AC-TiO_2 were 0.97, 0.26 and 0.43 cm^3/g; the average pore diameters were approximately 52, 20 and 55 Å (55.22, 3.0 and 5.5 nm) respectively.

Table 1 Textural Properties of Catalysts' Support Materials: AC, TiO_2 and AC-TiO_2

Catalysts' supports	BET Surface Area (m^2/g)	External Surface Area (m^2/g)	Micropore Area (m^2/g)	Total pore volume of pores (cm^3/g)	Average pore diameter (Å)
AC	583.3670	350.1640	233.2031	0.979245	52.3220
TiO_2	354.4782	349.9376	4.5405	0.263163	29.6959
AC-TiO_2	310.5169	219.1774	91.3395	0.432088	55.6604

The average pore diameters of the three catalysts are further indications that all the support materials are mesoporous since the values are all greater than 2 nm and less than 50 nm [100] and [3]. Moreover, the N_2 adsorption-desorption isotherms of the all the prepared support materials are similar to the type-IV isotherm exhibited by mesoporous materials. The N_2 adsorption-desorption isotherms for AC, TiO_2, and AC-TiO_2 are presented in Figures 1, 2 and 3. The shapes of the of the isotherm for AC and TiO_2 are similar but there is a slight distortion in the case of AC-TiO_2 difference in the amount of N_2 adsorbed in each case. The observed distortion in the shape of AC-TiO_2 N_2 adsorption-desorption isotherm could be considered a reflection of the composite nature of the support material comprising both AC and TiO_2.

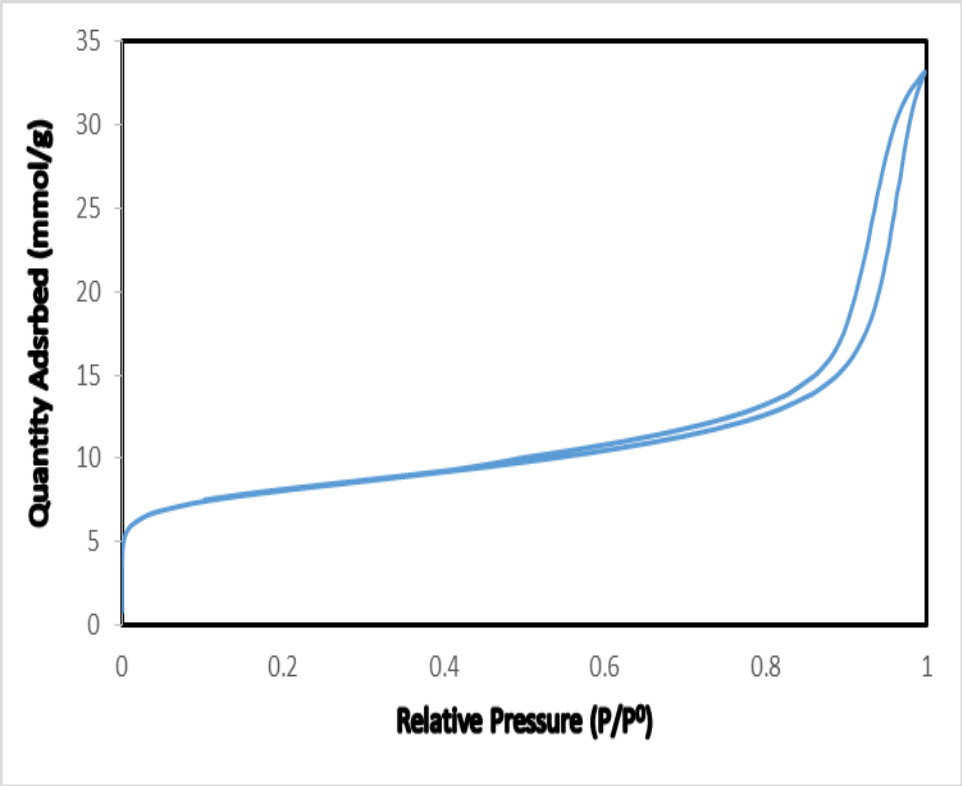

Figure 1. N_2 adsorption–desorption isotherms for /AC

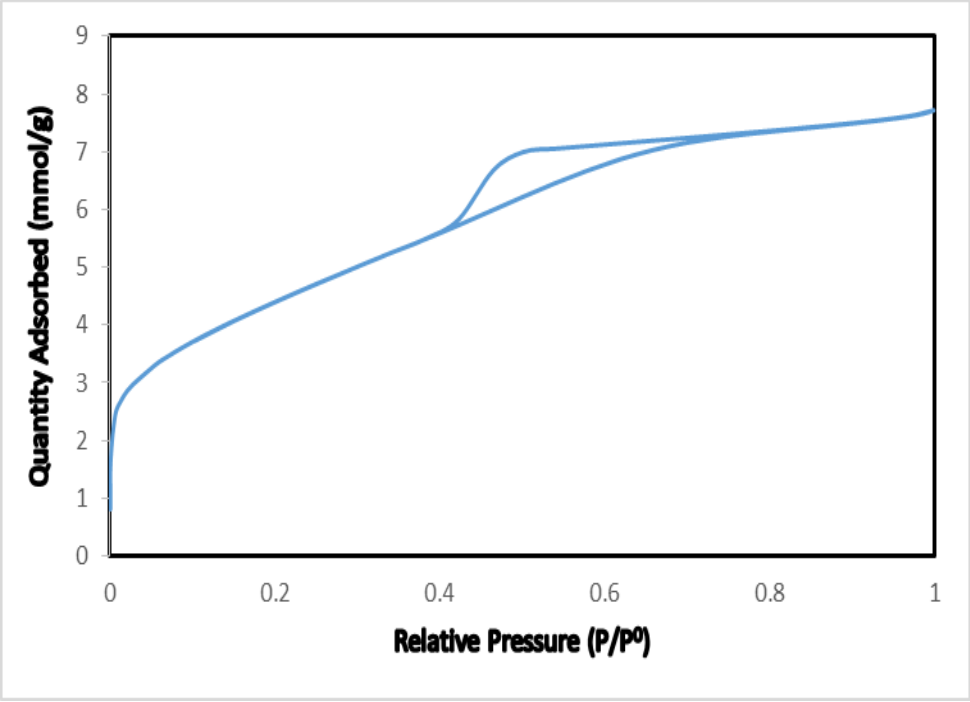

Figure 2. N_2 adsorption–desorption isotherms for TiO_2

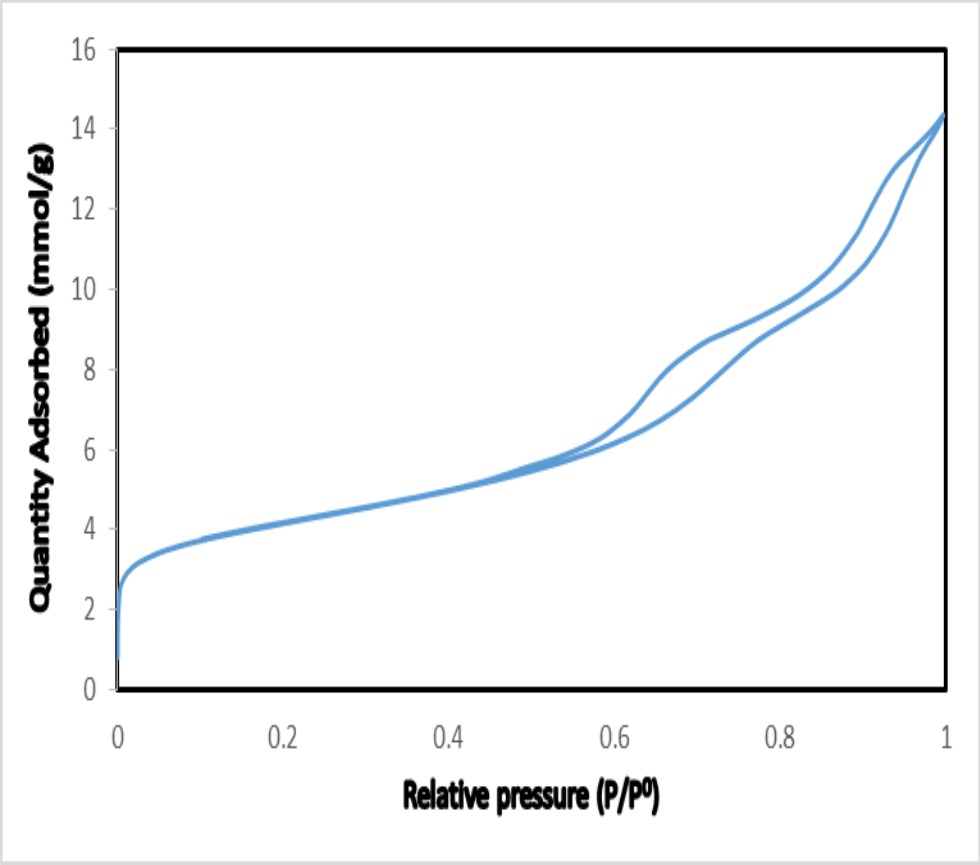

Figure 3. N_2 adsorption–desorption isotherms for AC-TiO_2

Textural properties of the catalysts supported on AC, TiO_2, and AC-TiO_2 are presented in Table 2. Analysis of the results shows that the textural properties of the support have changed on loading the supports with equivalent amounts of metal catalyst. A reduction the BET surface, external surface area and micropore area of the support materials can be observed when the values in Table 2 and Table 3 are compared. For example, the surface BET surface is of AC is reduced to 352 m^2/g from 583 m^2/g on loading the Ni and Mo metal species onto the support material to form the corresponding NiMo/AC catalyst. A similar trend of reduction in BET surface area is observed when results obtained for TiO_2 and AC-TiO_2 are compared against the corresponding catalysts, NiMo/TiO_2 and NiMo/AC-TiO_2 respectively. The observed reduction in the BET surface area, external surface area, micropore area, and the total pore volume of the of the support materials, when compared to the corresponding HDS catalysts, is a result of the successful incorporation of the metal catalysts onto the support materials.

Table 2. Textural Properties of Catalysts: NiMo/AC, NiMo/TiO_2, and NiMo/AC-TiO_2

Catalysts	BET Surface Area (m^2/g)	External Surface Area (m^2/g)	Micropore Area (m^2/g)	Total pore volume of pores (cm^3/g)	Average pore diameter (Å)
NiMo/AC	352.1114	230.7778	121.3336	0.530329	60.2456
NiMo/TiO_2	225.82	220.98	2.633	.3218	31.751
NiMo/AC-TiO_2	220.8506	170.6991	50.1515	0.475779	86.1721

Another interesting observation the change in the overage pore size of the support materials on the incorporation of the metal catalysts. The average pore diameters of AC and TiO_2 and AC-TiO_2 increased from the initial values of 52 Å (5.2 nm), 30 Å (3.0 nm) to 60 Å (6.0 nm) 31 Å (3.1 nm) and 86 Å (8.6nm), respectively, after the impregnation with Ni and Mo species. The observed increase in pore diameter could be attributed to the occupation or blocking of some of the micro pores on the of the support materials by the metal Nano particles. Thus, leading to a decrease in the proportion of the micro pores compared to the mesopores. Moreover, it is clear from the shape of the N_2 adsorption-desorption isotherms of the catalyst, NiMo/AC, NiMo/TiO_2 and NiMo/AC-TiO_2 , presented in Figures 4, 5, and 6 that the prepared materials are mesoporous.

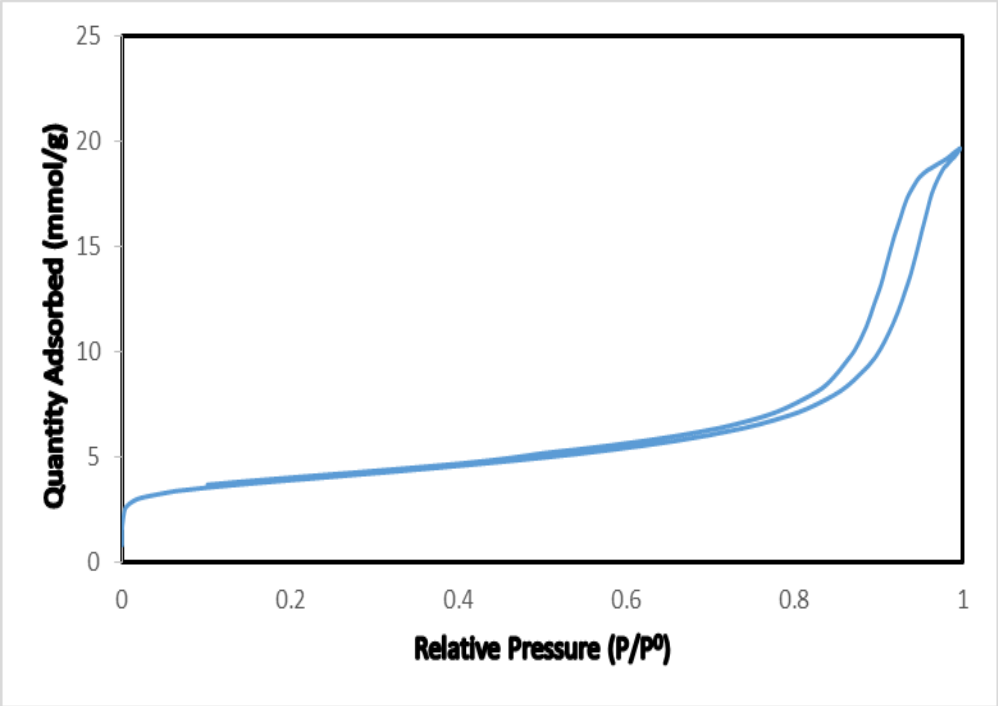

Figure 4. N_2 adsorption–desorption isotherms for NiMo/AC-TiO_2

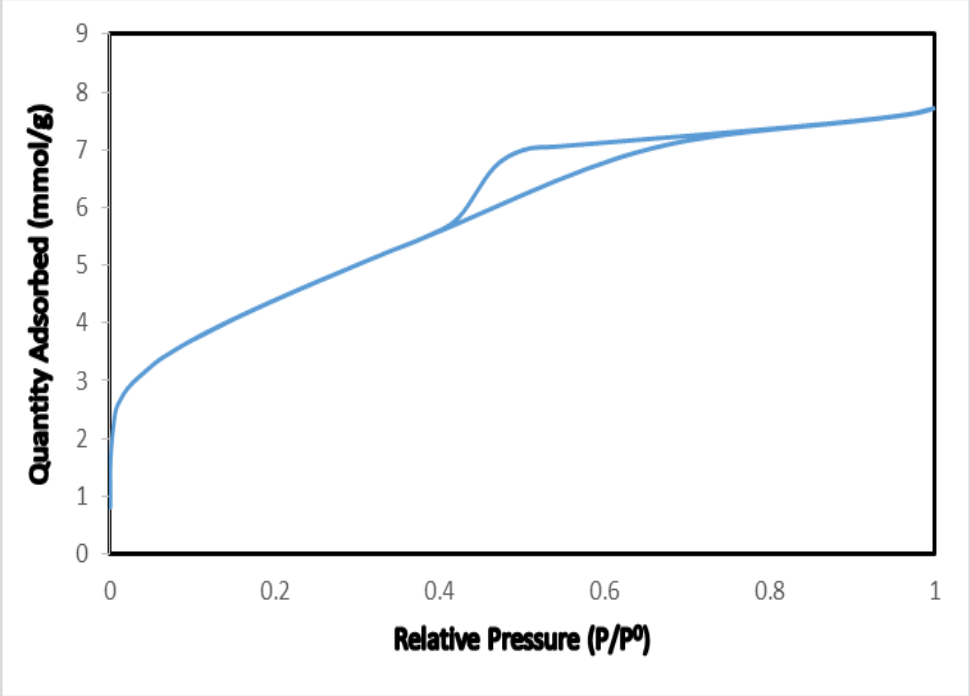

Figure 5. N_2 adsorption–desorption isotherms for $NiMo/TiO_2$

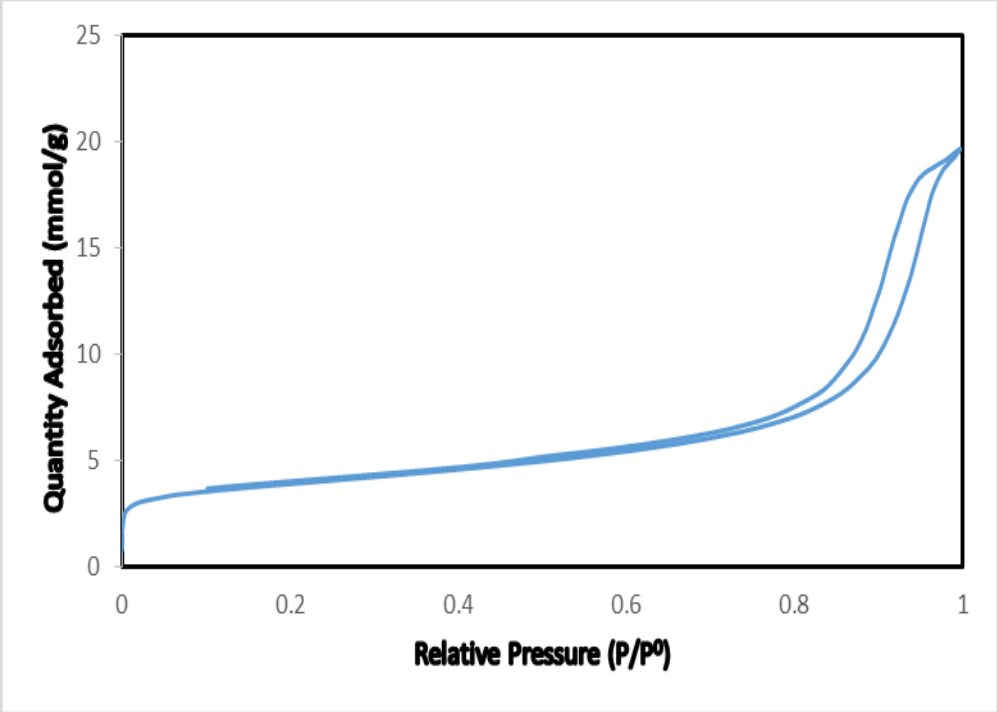

Figure 6. N_2 adsorption–desorption isotherms for $NiMo/AC\text{-}TiO_2$

Results for the textural properties of NiMo/AC100, NiMo/AC200, NiMo/AC300 and NiMo/AC400 are presented in Table. 3 Besides the fact that the that the textural properties of the carbon support changed on loading the supports with the metal catalysts, analysis of the results show and there is a correlation between the calcination temperature at which the prepared catalysts were treated after impregnation. NiMo/AC400 has the largest BET surface area of 434.5 m^2/g and the difference is very significant when compared with 323 352 and 356 m^2/g which are the obtained for NiMo/AC100, NiMo/AC200 and NiMo/AC300 respectively. A similar trend is observed for the external surface area and micropore area as well as the pore volumes of the supported HDS catalyst. The observed phenomena can be a result of the fact that more effective evacuation of the adsorbed H_2O molecule trapped within the pores of the carbon support

Table 3 Textural Properties of Catalysts: NiMo/AC100, NiMo/AC200 and NiMo/AC300 NiMo/AC400

Catalysts	BET Surface Area (m^2/g)	External Surface Area (m^2/g)	Micropore Area (m^2/g)	Total pore volume of pores (cm^3/g)	Average pore diameter (Å)
NiMo/AC100	323.0251	220.0663	102.9588	0.529609	65.5811
NiMo/AC200	356.6956	229.1308	127.5647	0.548710	61.5325
NiMo/AC300	352.1114	230.7778	121.3336	0.530329	60.2456
NiMo/AC400	434.5335	259.5915	174.9420	0.595631	54.8295

The N_2 adsorption-desorption isotherms for NiMo/AC100, NiMo/AC200, NiMo/AC300, NiMo/AC400 are presented in Figures 7, 8, 9 and 10 respectively. The shapes of the isotherms are similar and match the type IV isotherms that is unique to the mesoporous material. Moreover, the average pore size (Table 4) of all the catalysts fall within the range 2 nm and 50 nm. The average pore size recorded for NiMo/AC100, NiMo/AC200, NiMo/AC300 and NiMo/AC400 are 66 Å (6.6 nm), 62 Å (6.2 nm), 60 Å (6.0 nm) and 55 Å (5.5 nm) respectively. It is important to note the decrease in the average pore size of the catalysts as the calcination temperature is increased from 100-400^{0}C. Though the difference in pore size might be considered small when the values for NiMo/AC100, NiMo/AC200, and NiMo/AC300 are compared but the difference becomes significant when the pore size of NiMo/AC400 is compared with the others.

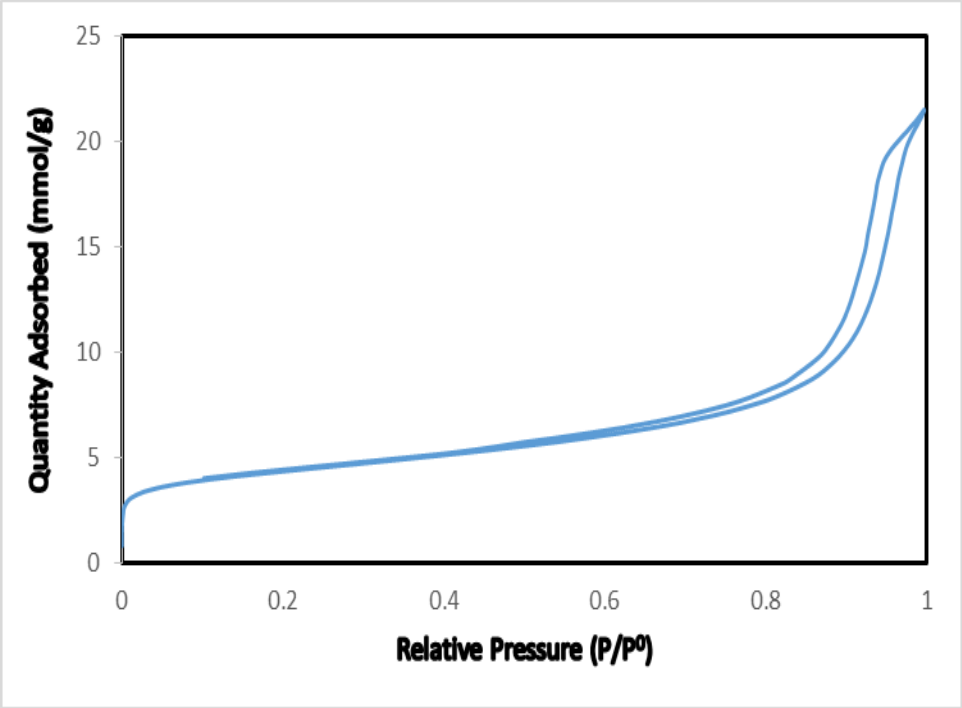

Figure 7. N_2 adsorption–desorption isotherms for NiMo/AC100

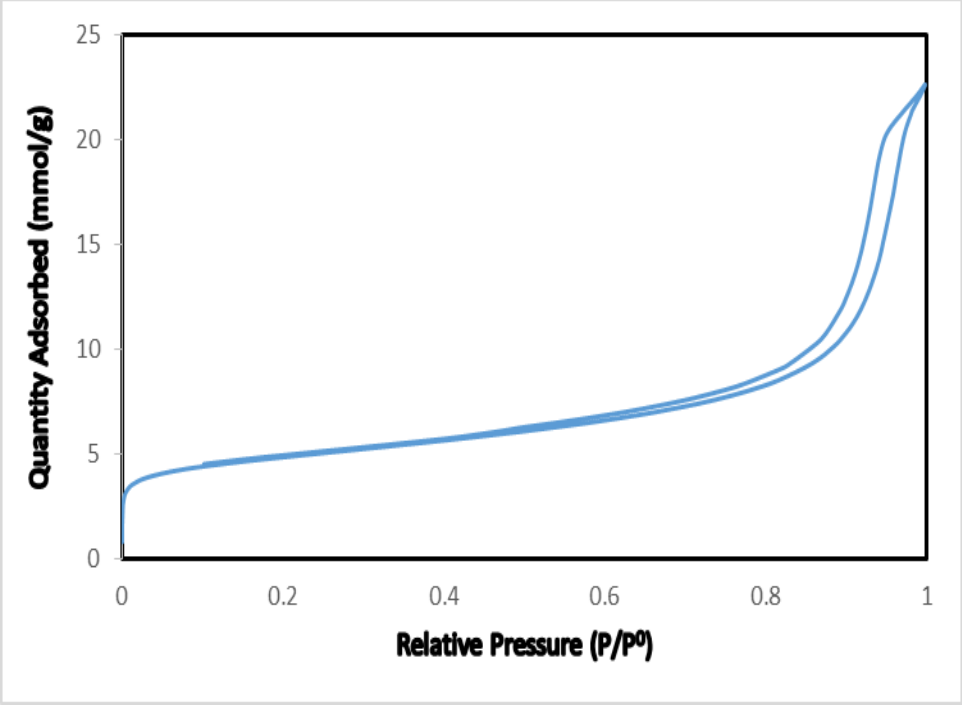

Figure 8. N_2 adsorption–desorption isotherms for NiMo/AC200

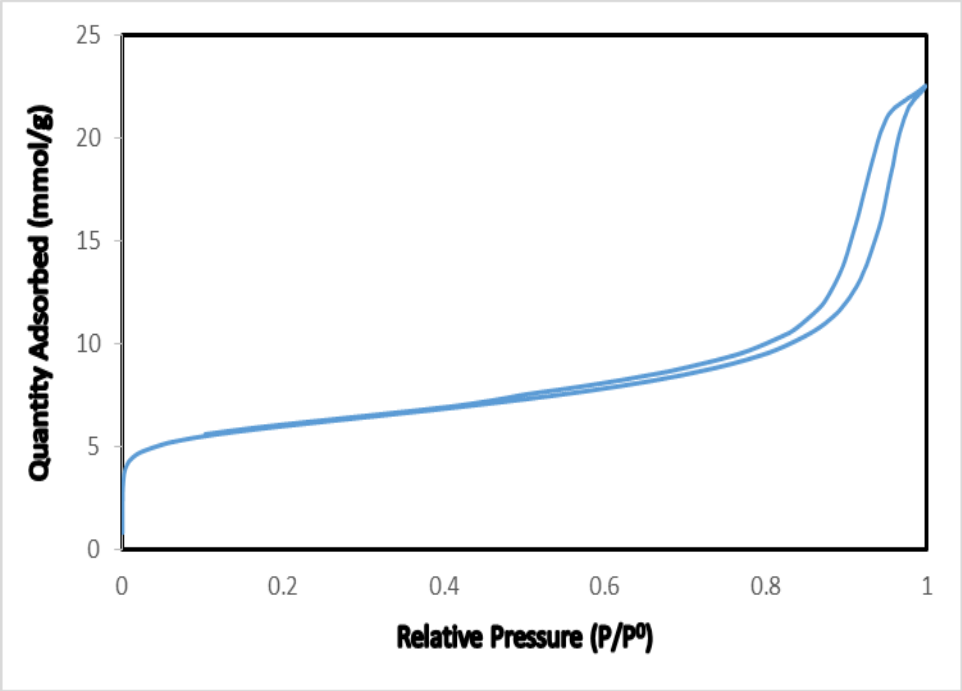

Figure 9. N_2 adsorption–desorption isotherms for NiMo/AC300

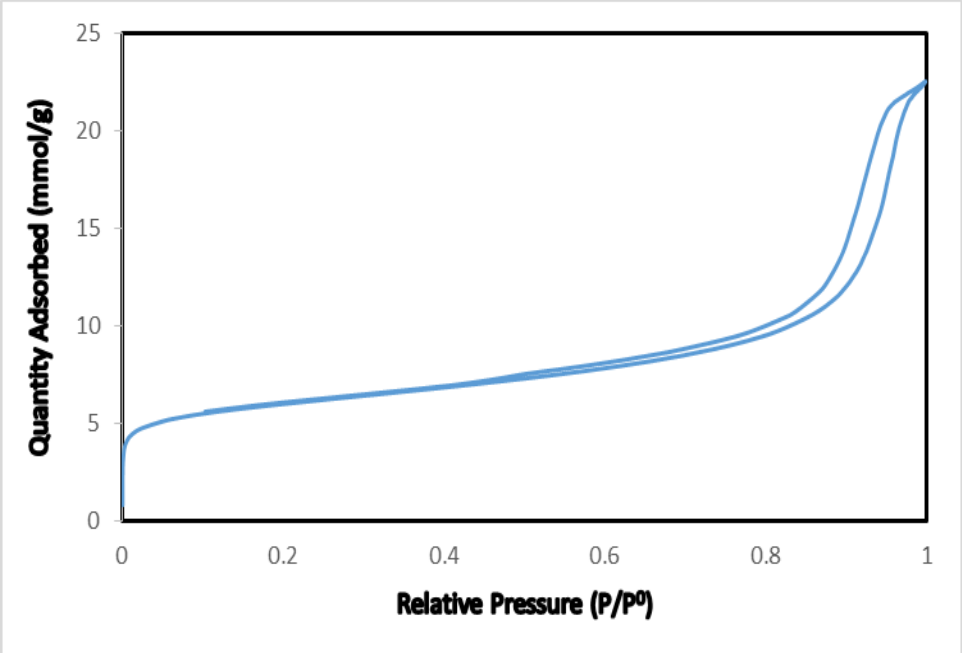

Figure 10. N_2 adsorption–desorption isotherms for NiMo/AC400

Results for the textural properties of NiMo/AC(U-S), NiMo/AC(CA) and NiMo/AC(EDTA) are presented in Table 4. The textural properties of the carbon support changed on loading the supports with the metal catalysts just in like the case of other catalysts discussed in the previous sections. Analysis of the results shows that there are differences in the measured BET surface area, external surface area, and micropore area and pore volume of the catalyst. NiMo/AC(EDTA) has the largest BET surface area of 342 m^2/g compared to the values of 278 and 288 m^2/g recorded for NiMo/AC(U-S), NiMo/AC(CA) respectively. A similar trend is observed for the external surface area and micropore area, as well as the pore volumes of the three, supported HDS catalyst. The observed differences could be due to the fact that the chelating agents, CA and EDTA could be more effectively evacuated from the surface of the pores compared to adsorbed water

Table 4 Textural Properties of Catalysts: NiMo/AC(U-S), NiMo/AC(CA) and NiMo/AC (EDTA)

Catalysts	BET Surface Area (m^2/g)	External Surface Area (m^2/g)	Micropore Area (m^2/g)	Total pore volume of pores (cm^3/g)	Average pore diameter (Å)
NiMo/AC(U-S)	278.7802	215.0349	85.7453	0.453232	61.1136
NiMo/AC(CA)	288.7802	205.0349	83.7453	0.441932	61.2136
NiMo/AC(EDTA)	342.8653	235.5285	107.3368	0.485952	56.6930

Besides the changes observed in the surface area and pore volumes of the prepared catalysts when compared to the activated carbon support, there are noticeable changes in the pore size of the materials. The pore diameter of the activated carbon support was 5.2 nm compared to the 5.7, 6.1 and 6.1 nm recorded for NiMo/AC(U-S), NiMo/AC(CA) and NiMo/AC(EDTA) respectively. The average pore diameters of NiMo/AC(CA) and NiMo/AC(EDTA) are the same but larger than the average pore diameter of NiMo/AC(U-S). This is an indication that both CA and EDTA had similar effects on the textural properties of the prepared catalysts and their impacts might be different compared to the use of ultrasonication. In all cases, the average pore diameters of the catalysts are between the range of 2 - 50 nm and it shows that the materials are mainly mesoporous. It is evident from the shape of the N_2 adsorption-desorption isotherms presented in Figures 11, 12 and 13, that the three catalysts are mesoporous as the shapes are similar to the type IV isotherms peculiar to the mesoporous material.

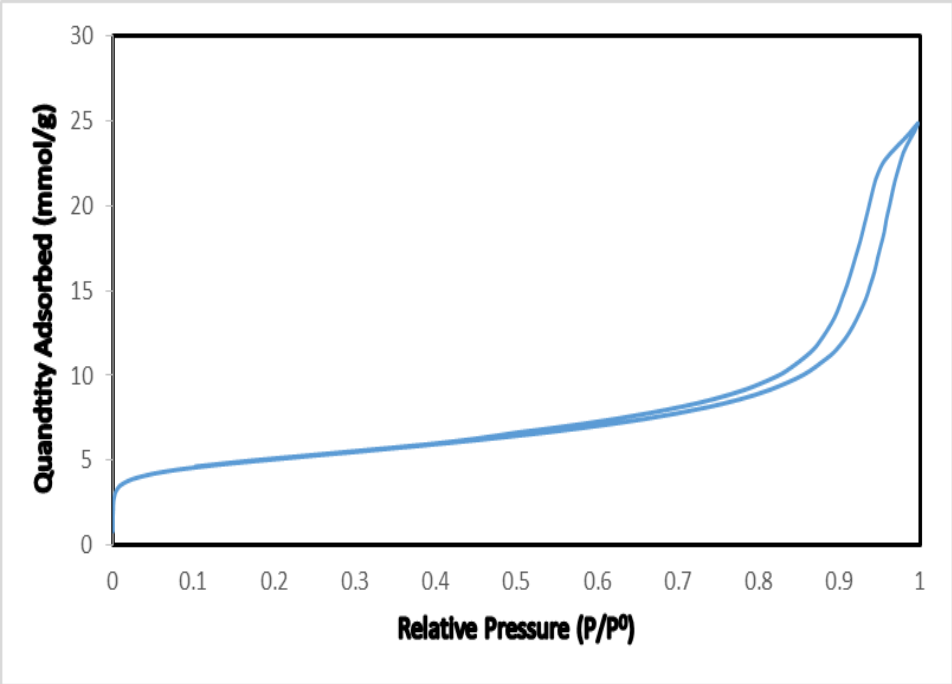

Figure 11. N_2 adsorption–desorption isotherms for NiMo/AC(US)

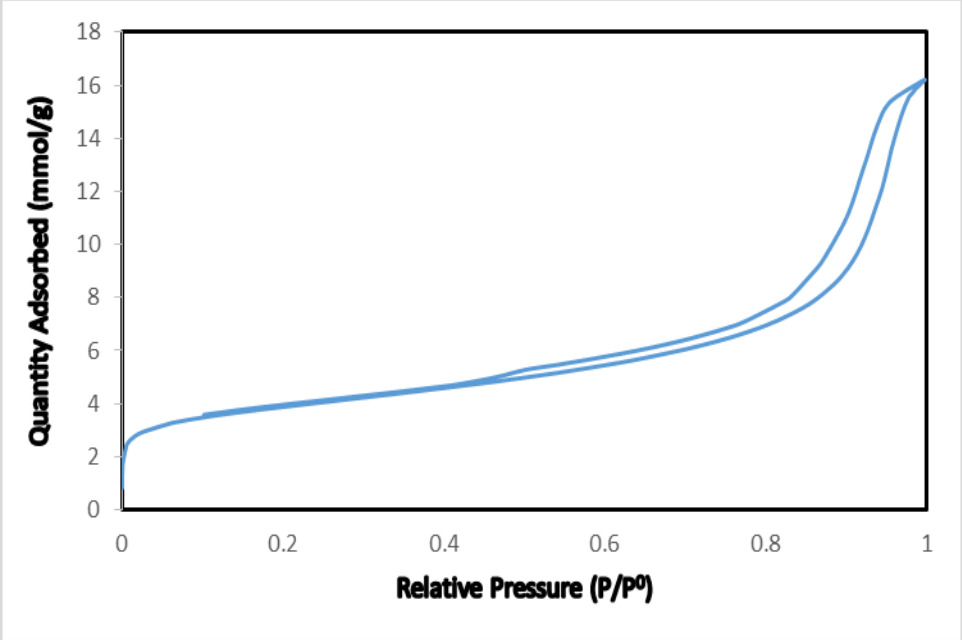

Figure 12. N_2 adsorption–desorption isotherms for NiMo/AC(CA)

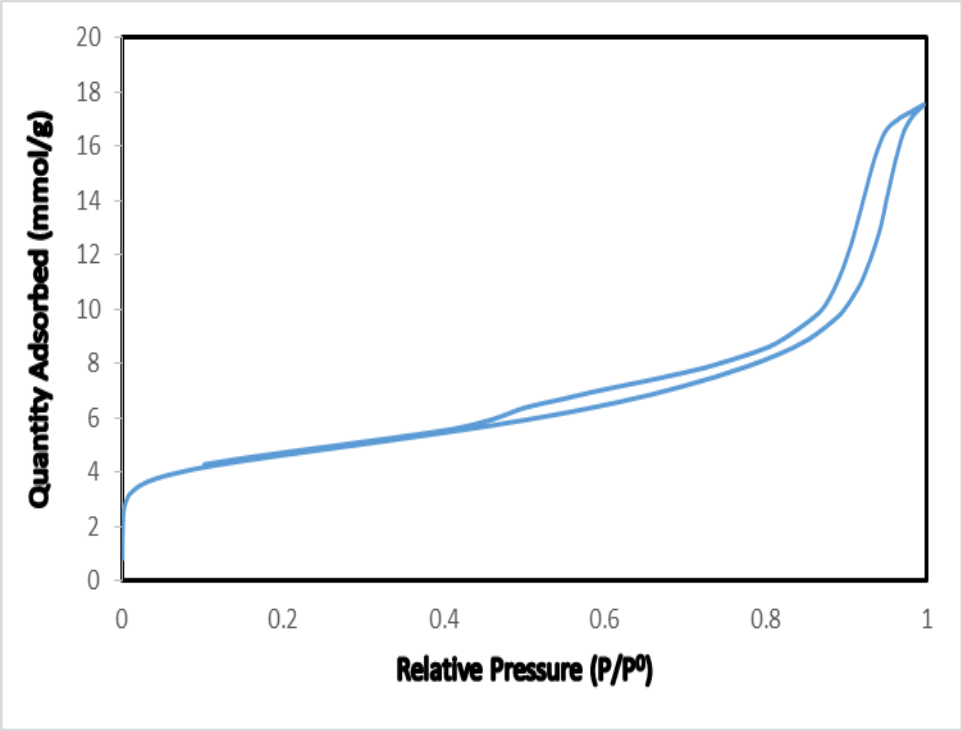

Figure 13. N_2 adsorption–desorption isotherms for NiMo/AC(EDTA)

4.1.2 FT-IR

The FTIR spectra shown in Figures 14 and 15 reveal some of the functional groups present in the supported catalysts. The most conspicuous are the bands centered around 3400, 2350, 1600 and 1300 -100 cm^{-1}. The broad band centered at 3400 cm^{-1} is peculiar to the stretching (O–H) vibration in compounds with hydroxyl groups while the band at 2350, 1600 and 1300 -100 cm^{-1} are unique to the to C≡C stretching vibration in alkyne group, (C═O) stretching vibrations of carboxylic and carbonyl compounds. This is a clear indication of the presence of acidic oxygen groups that can serve as adsorption sites on the surface of the catalysts. Peaks can be attributed to the Mo-O-Mo stretching vibrations are found at 620 and 850 cm^{-1} while the band at 797 cm^{-1}can be conveniently attributed to the presence of the polymobdate species, Mo_{36}.

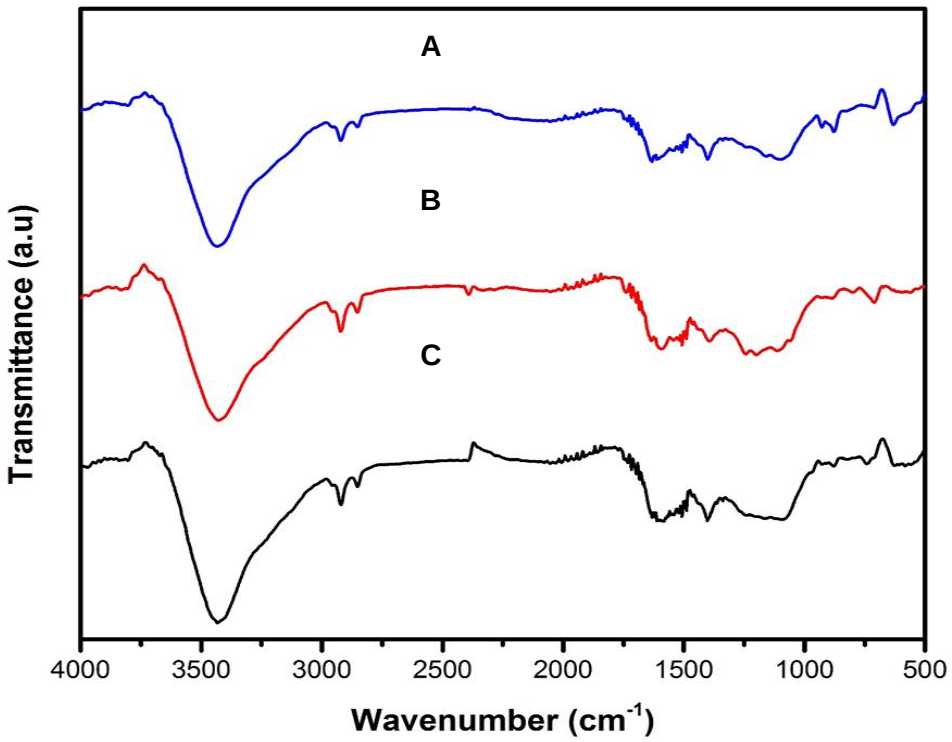

Figure 14. FT-IR Spectra: (A) NiMo/AC(U-S), (B) NiMo/AC(CA) and (C) NiMo/AC(EDTA).

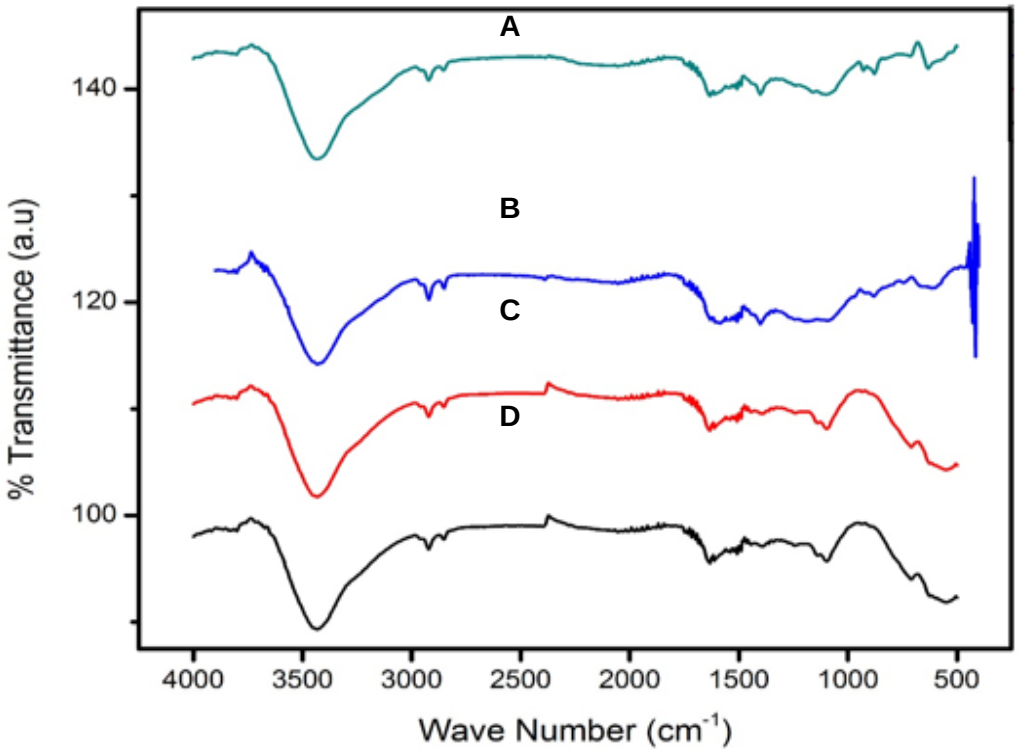

Figure 15. FT-IR Spectra: (A) NiMo/AC100, (B) NiMo/AC200 and (C) NiMo/AC300 and (D) NiMo/AC400.

4.1.3 XRD

The powder X-ray diffraction results for the catalysts NiMo/AC100, NiMo/AC200, NiMo/AC300 and NiMo/AC400 are presented in Figure 16. The diffractograms are stacked for ease of comparison. In all cases, there are three major broad diffraction peaks at 2θ values of 25^{o}, 37^{o} and 54^{0}. However, the peaks for NiMo/AC300 and NiMo/AC400 are more intense when compared to NiMo/AC100 and NiMo/AC200. The appearance of these peaks can be attributed to presence of Mo species and the varying degree of intensity of the peaks is a result of the difference in degree of crystallinity. This an indication that the calcination at high affects the degree of crystallinity of Mo incorporated into the carbon support. The other peaks are broad and barely visible but the most conspicuous diffraction peak at around 2θ 25^{0} can be be attributed to the hexagonal MoO_3 [101]–[103]. diffraction peaks at 2θ values 20^{0}-30^{0} (002) 40^{o} to 50^{o} (101) have been reported for the graphite phase of activated carbon[104]–[106]. The additional peaks can be attributed to the other forms MoO_3 or even MoO_2. Therefore the presence of these peaks can be taken as additional evidence of successful impregnation of the carbon support with the metal catalyst. There are no visible and peculiar peaks that indicate the presence of and Ni due to the low concentration of the promoter compared to the proportion Mo. [107].

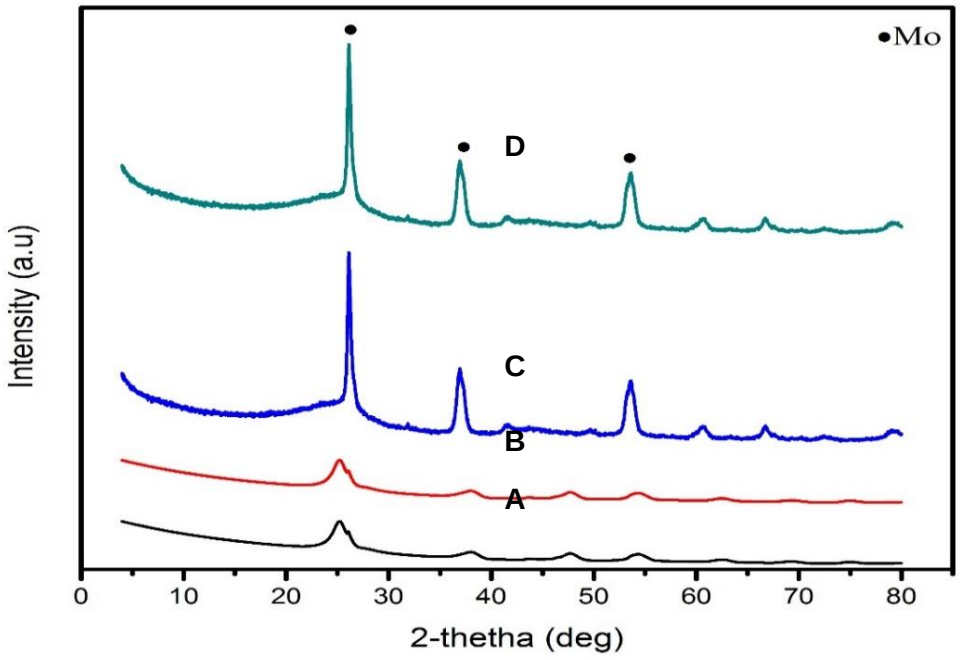

Figure 16. X-Ray Dffractograms: (A) NiMo/AC100 , (B) NiMo/AC200 and (C) NiMo/AC300 (D)NiMo/AC400.

4.1.4 SEM and EDX

The scanning electron microscopy (SEM) images in Figures 17 and 18 show surface morphology and textural characteristics of selected catalysts. It important to note that the particles are do not have a regular shapes but it is a common feature of activated carbon and other amorphous materials used as adsorbent or as catalysts support. [58]. Other porous materials like MOFs SBA-15 that are often used as support and adsorbents have characteristic shapes and distinct morphology. It is obvious that some of the pores on the surface of the activated carbon support as well as metal particles on the surface are visible - an indication that some of the metals got deposited onto the surface of the carbon support and the others might be trapped the pores. Figure 19 is the energy dispersive x-ray (EDX) spectra, and Table 5. It provides both qualitative and quantitative information about the surface composition of the prepared catalysts. The identified elements present carbon and oxygen, molybdenum, cobalt and nickel. It was not unexpected that carbon has the most intense peak and it represent over sixty percent of the elements since it the main component element of the support material. The oxygen and molybdenum peaks are also conspicuous and accounts for approximately nine percent and seven percent respectively. The above is a clear indication that the Mo, Co and Ni were Nano particles were successfully incorporated onto the activated carbon support.

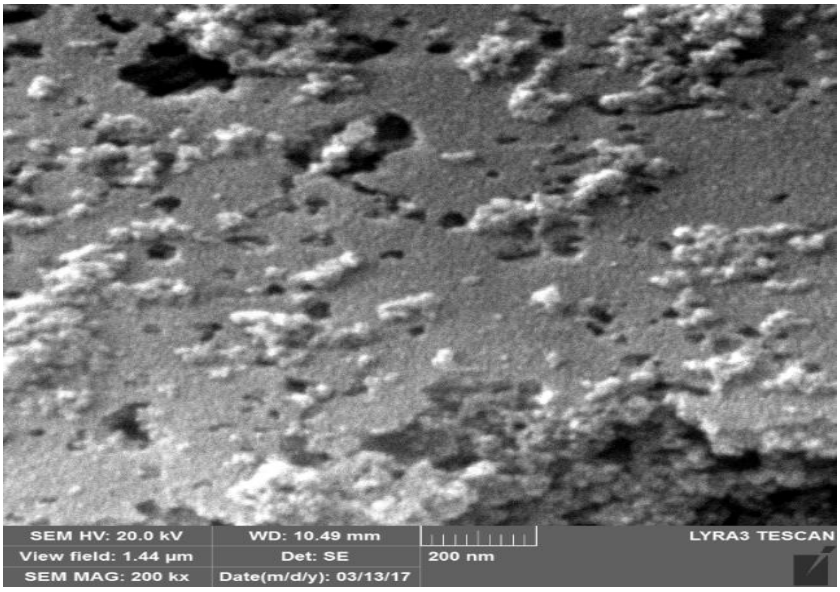

Figure 17. SEM Images of NiMo/AC

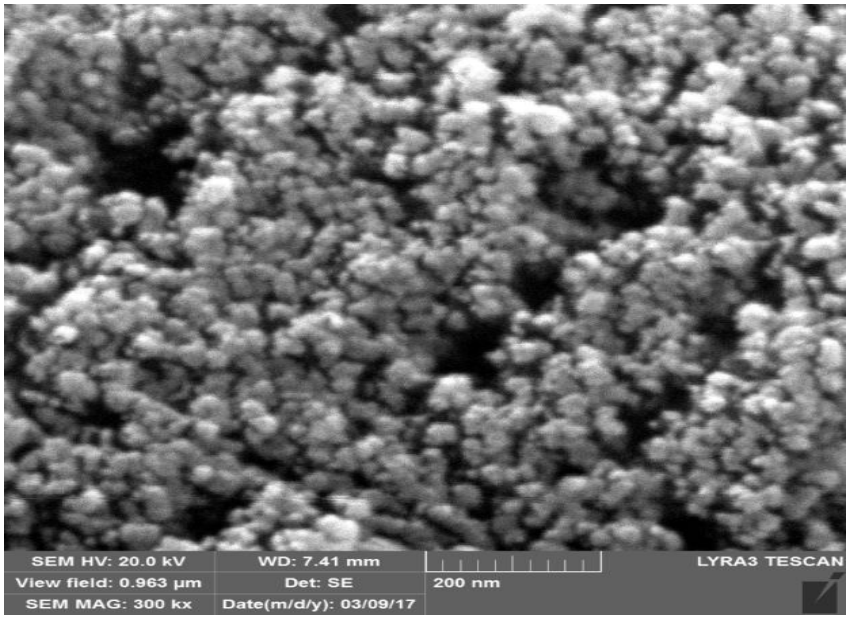

Figure 18. SEM Images of NiMo/AC

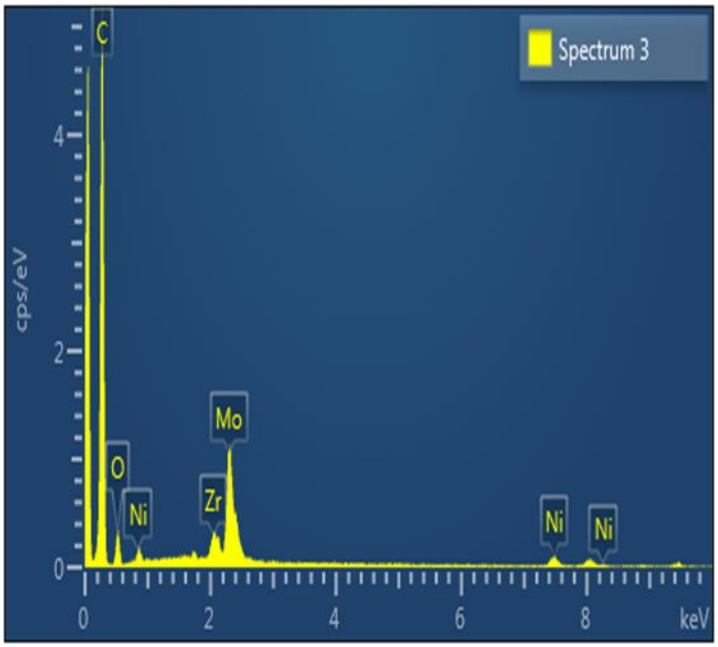

Figure 19. EDX spectra of NiMo/AC

Table 5. Distribution of elements on the surface of the NiMo/AC

Element	Line Type	Apparent Concentration	k Ratio	Wt%	Wt% Sigma
C	K series	66.46	0.66463	81.81	0.54
O	K series	5.89	0.01982	9.02	0.49
Ni	K series	3.55	0.03547	1.52	0.13
Zr	L series	0.00	0.00000	0.00	0.00
Mo	L series	17.10	0.17096	7.64	0.27
Total:				100.00	

4.2 HDS Activity of Catalysts

4.2.1 Nature Support Materials and HDS Activity

The performance of the prepared catalysts towards the desulphurization of DBT for the reactions conducted in a pressure batch reactor are presented in Table 6 and Figure 20. In all cases, a continuous decrease in the concentration of the DBT in the model fuel was observed as the reactions progress. There was a decrease in the concentration of DBT even at the zeroth hour when sampling begins, an indication that the hydrodesulphurization reaction starts before the reaction temperature reaches the desired set point of 350^{o}C. Earlier reports have shown that HDS of DBT is feasible even at lower temperatures of 300^{o}C using the Mo based catalysts supported on carbon [108].

When the concentration of DBT in samples collected at the same interval for the three catalysts are compared, it was observed that the centration are not the same. The concentration of the DBT was consistently lower in the case of NiMo/AC than when NiMo/TiO_2 and NiMo/AC-TiO_2 were used as catalysts for the HDS reaction. The relative difference performance can be attributed to the nature of the support material since the amounts of the Ni and Mo on the materials are the same. The obvious advantage the carbon material has over the TiO_2 is the larger surface area and perhaps the differences in the pore structure. Previous studies have shown higher conversions can be achieved using materials with larger surface area [109]–[111]. Moreover, comparison of the carbon materials and metal oxides have shown that materials with a large surface are performed better than TiO_2 Al_2O_3 [112] ,[16]. Another important observation is the performance of NiMo/TiO_2 when compared to NiMo/AC-TiO_2. A lower concentration of the DBT was recorded NiMo/AC-

TiO_2 at all the time intervals. Thus, it is clear that the carbon from waste tires is a more effective support material for the Ni and Mo when compared to TiO_2 and the composite material AC-TiO_2.

Table 6. HDS Test Results: Performance of NiMo/AC, NiMo/TiO_2 and NiMo/AC-TiO_2

Catalysts	Concentration of DBT in Products Sampled at intervals (ppm)			
	Set Point (0h)	1h	2h	3h
NiMo/AC	740	491	266	109
NiMo/TiO_2	607	465	391	228
NiMo/AC-TiO_2	795	423	220	62

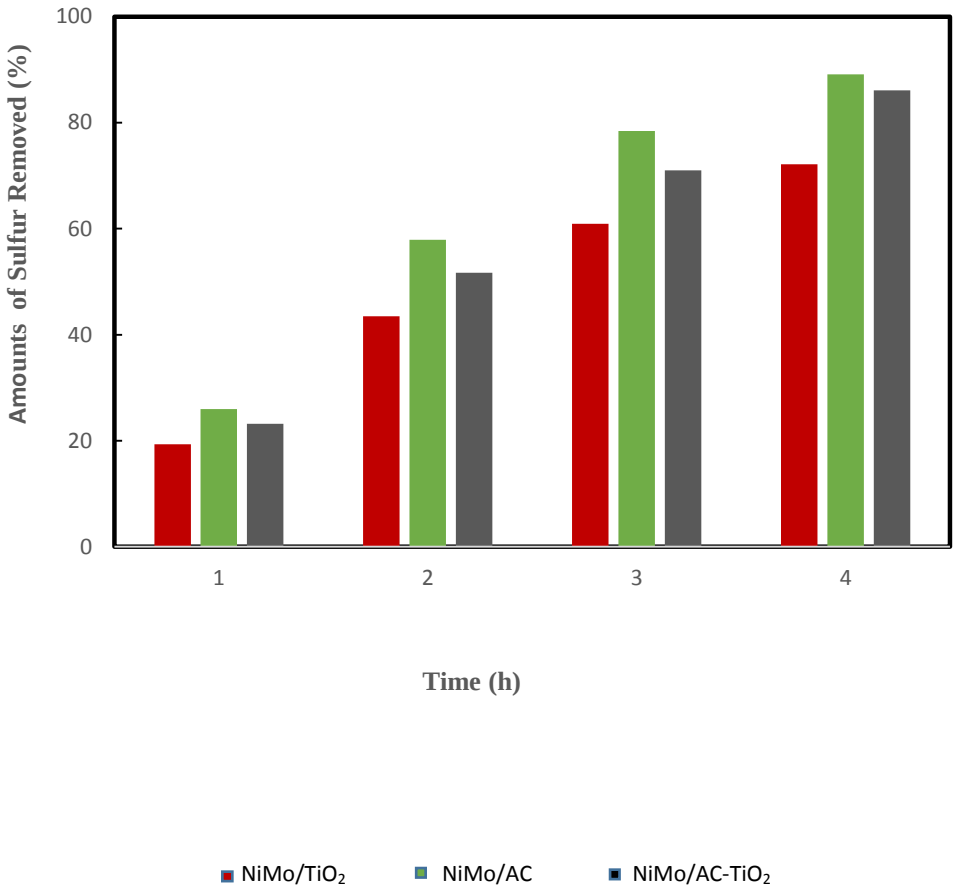

Figure 20. Amounts of sulfur removed using $NiMo/TiO_2$, NiMo/AC, and $NiMo/AC\text{-}TiO_2$

The HDS rate constants k (s^{-1}), k ($s^{-1}g^{-1}$cat.) and R^2 values were calculated for NiMo/AC, $NiMo/TiO_2$ and $NiMo/AC\text{-}TiO_2$ and the results presented in Table 7 and Figure 21. The magnitude of the R^2 values range from 0.850 to 0.989, an indication that the reactions involving all the tested catalysts agree well with the proposed pseudo-first order kinetics for the desulfurization process using supported Mo catalysts [113]. Calculations for the nth order rates yielded lower R^2 values. The results also show a strong correlation between the performance of the catalysts towards the desulfurization of DBT and the magnitude of the pseudo 1^{st} order rate constants. For example, the HDS rate constant for NiMo/AC(EDTA),

NiMo/AC(CA), NiMo/AC(U-S) and NiMo/AC are is 2.3×10^{-4} s^{-1}, 1.8×10^{-4} s^{-1}, 1.6×10^{-4} s^{-1} and 1.5×10^{-4} s^{-1} respectively. The differences in the magnitude of the HDS rate constants reflect the relative performance of the catalysts and, therefore, provides more insight into the activity of the prepared catalysts. It is now clear that NiMo/AC(EDTA) is most effective of the prepared and tested catalysts in the degradation of DBT. The magnitude of the HDS rates constants also indicates that the chelating agents are more effective in the dispersion of active metal species when compared to ultrasonication.

Table 7. Kinetic parameters: HDS Rate constants for NiMo/AC, NiMo/TiO_2 and NiMo/AC-TiO_2

Catalysts	1st Order Kinetics Rate Constants			
	k_{HDS} (s^{-1})	$k_{HDS}\times10^4$ (s^{-1})	$k_{HDS}\times10^4$ ($s^{-1}g^{-1}cat$)	R^2
NiMo/AC	2.0E-04	2.0E+00	6.58	0.988
NiMo/TiO_2	1.0E-04	1.00	3.33	0.965
NiMo/AC-TiO_2	1.7E-04	1.73	5.75	0.985

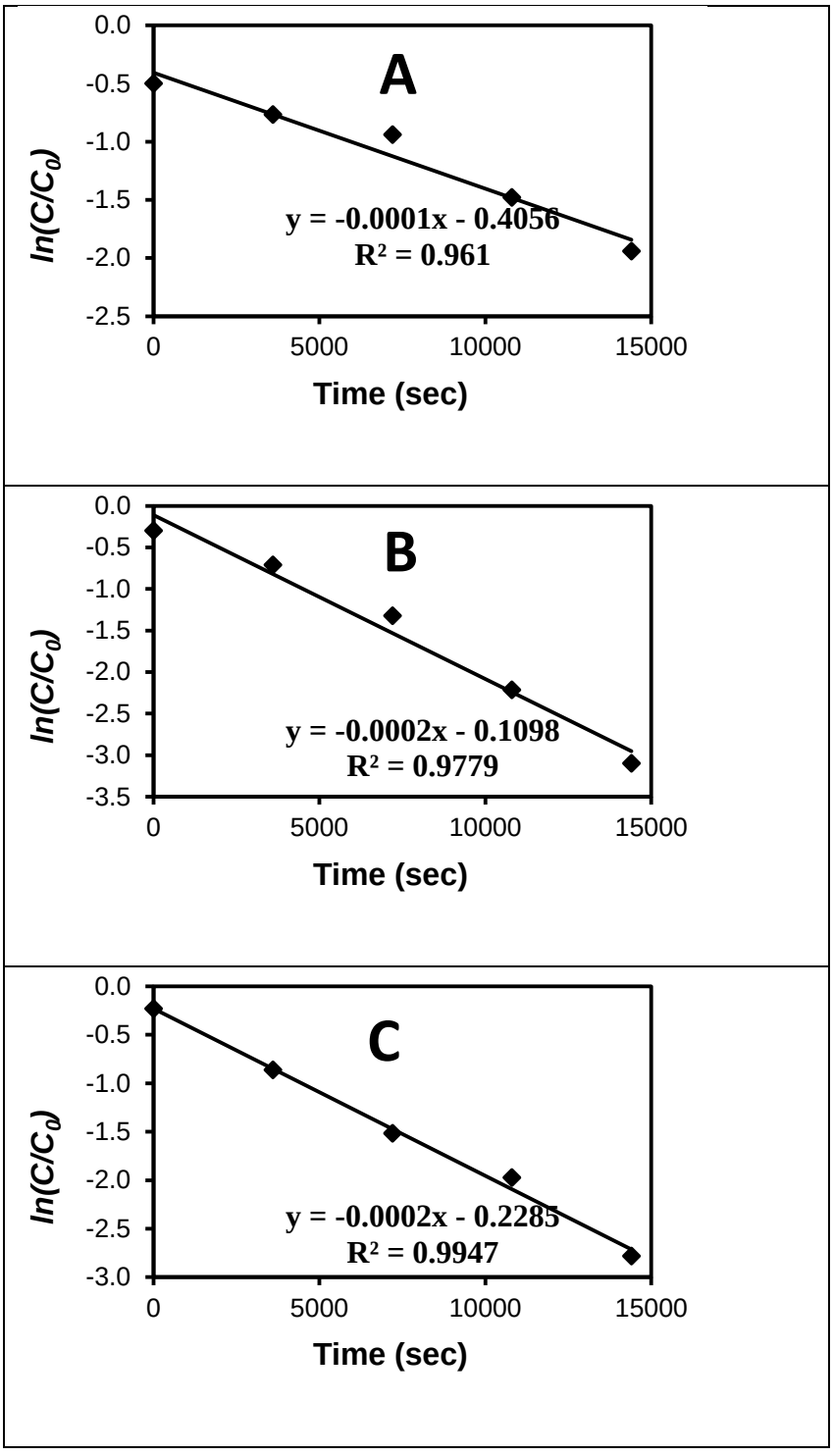

Figure 21. Kinetic plots of (A) NiMo/ TiO_2 (B) NiMo/AC-TiO_2 and (C) NiMo/AC

4.2.2 Effects of Calcination Temperature

The results in Table 8 and Figure 22 show the concentration of sulfur present in the model at various during the reaction when the catalysts NiMo/AC100, NiMo/AC200 and NiMo/AC300 and NiMo/AC400 were used. The differences concentration of sulfur at the same time intervals using the catalysts calcined at a different temperature is an indication that the activity of the catalysts was affected by the thermal treatment. Considering the concentration profiles of the products collected at the different hours of the experiments clearly shows that the catalysts calcined at 100 and 200^0C to be more effective in the HDS of DBT. There is a significant difference between the sulfur concentration of products of samples collected at the same time even though the catalysts, are prepared from the same materials and under the same conditions except for calcination temperature. Thus it would be rational to attribute the difference in activity of the catalysts to modifications that occur during the calcination process. Perhaps some functionalities and features that facilitate the operation of the catalyst are lost at higher calcination temperature. Recent studies on NiMo supported on SBA-15 showed that higher activity is achieved when the catalysts were calcined at 300^{o}C than at higher temperatures [114]. It is obvious that the two catalysts, CMAC and NMAC, also perform better when treated at 300^{o}C and the difference in activity is not very significant when the two catalysts calcined at the same temperature.

Table 8. HDS Test Results: Performance of NiMo/AC100, NiMo/AC200, NiMo/AC300 and NiMo/AC400

Catalysts	Concentration of DBT in of products taken at intervals (ppm)			
	Set point (0h)	1h	2h	3h
NiMo/AC100	713	546	112	49
NiMo/AC200	740	512	122	60
NiMo/AC300	882	658	385	147
NiMo/AC400	840	691	366	153

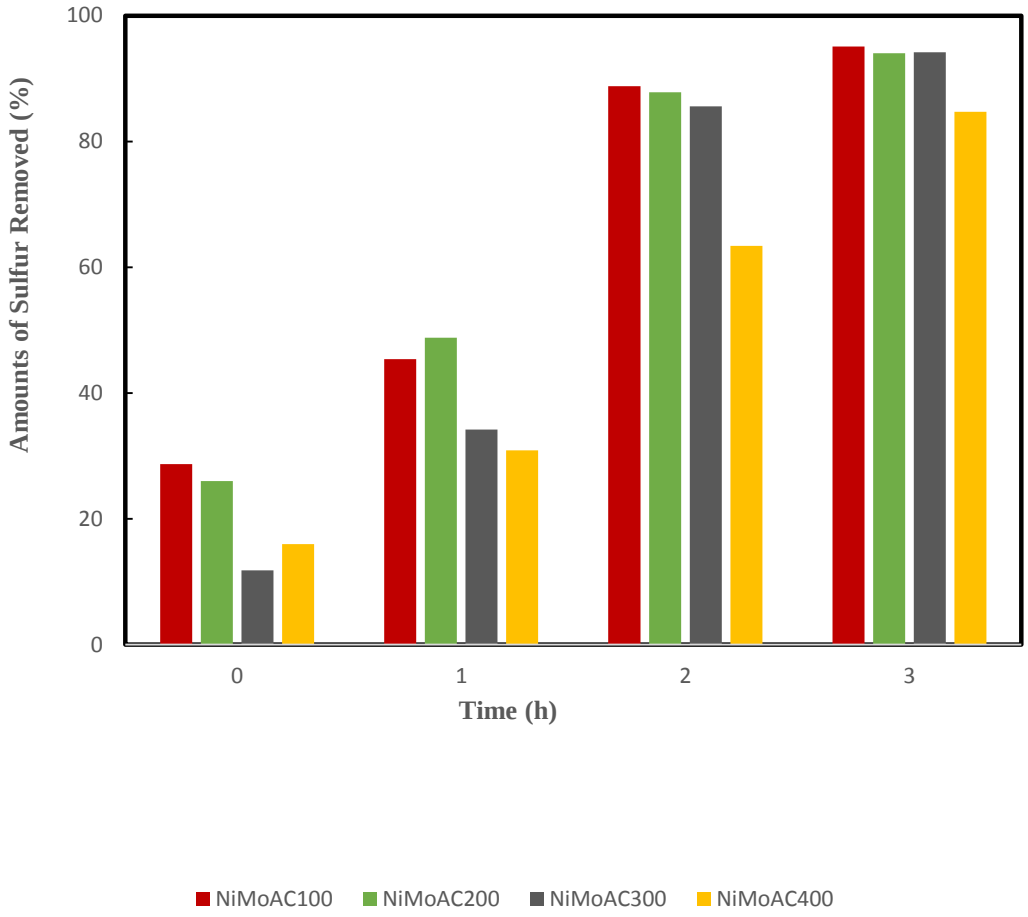

Figure 22. Amounts of sulfur removed using NiMo/AC100 NiMo/AC200 NiMo/AC300 and NiMo/AC400

The HDS rate constants k (s^{-1}), $ks^{-1}g^{-1}cat$. R^2 values were calculated for all the prepared catalysts, catalysts NiMo/AC100, NiMo/AC200 and NiMo/AC300 and NiMo/AC400, and the results are presented in Table 9. The values were determined using the initial conversion values – those obtained after the first hour of the reaction. The magnitude of the R^2 values range from 0.850 to 0.989, an indication that the reactions involving all the tested catalysts agree well with the proposed pseudo-first order kinetics for the desulfurization process using supported Mo catalysts. Calculations for the nth order rates yielded lower R^2 values

A similar trend is observed in the relative magnitude of the catalysts subjected to thermal treatments at different temperatures prior to the reduction, presulfidation, and the subsequent activity HDS activity tests as described in the previous sections. The pseudo 1^{st} order rate constant calculated for NiMo/AC100, NiMo/AC200, NiMo/AC300 and NiMo/AC400 are 2.0×10^{-4}, s^{-1} 1.9×10^{-4} s^{-1}, 8.8×10^{-5} s^{-1} and 8.9×10^{-5} s^{-1} respectively, Figure 23. The decrease in the magnitude of the rate constant as the calcination temperature increases is a clear indication that calcination at higher temperatures reduces the activity of the catalyst. The observed phenomenon can be attributed to the increase the crystallinity of the active species as evident in the XRD spectra.

Table 9. Kinetic parameters: HDS Rate constants for NiMo/AC100 NiMo/AC200 NiMo/AC300 and NiMo/AC400

Catalysts	1st Order Kinetics Constants			
	k_{HDS} (s^{-1})	$k_{HDS}\times10^4$ (s^{-1})	$k_{HDS}\times10^4$ ($s^{-1}g^{-1}cat$)	R^2
NiMo/AC100	2.0E-04	1.52	5.05	0.972
NiMo/AC200	1.9E-04	1.9E+00	6.18	.997
NiMo/AC300	8.8E-05	0.88	2.92	0.980
NiMo/AC400	8.9E-05	0.89	2.97	0.989

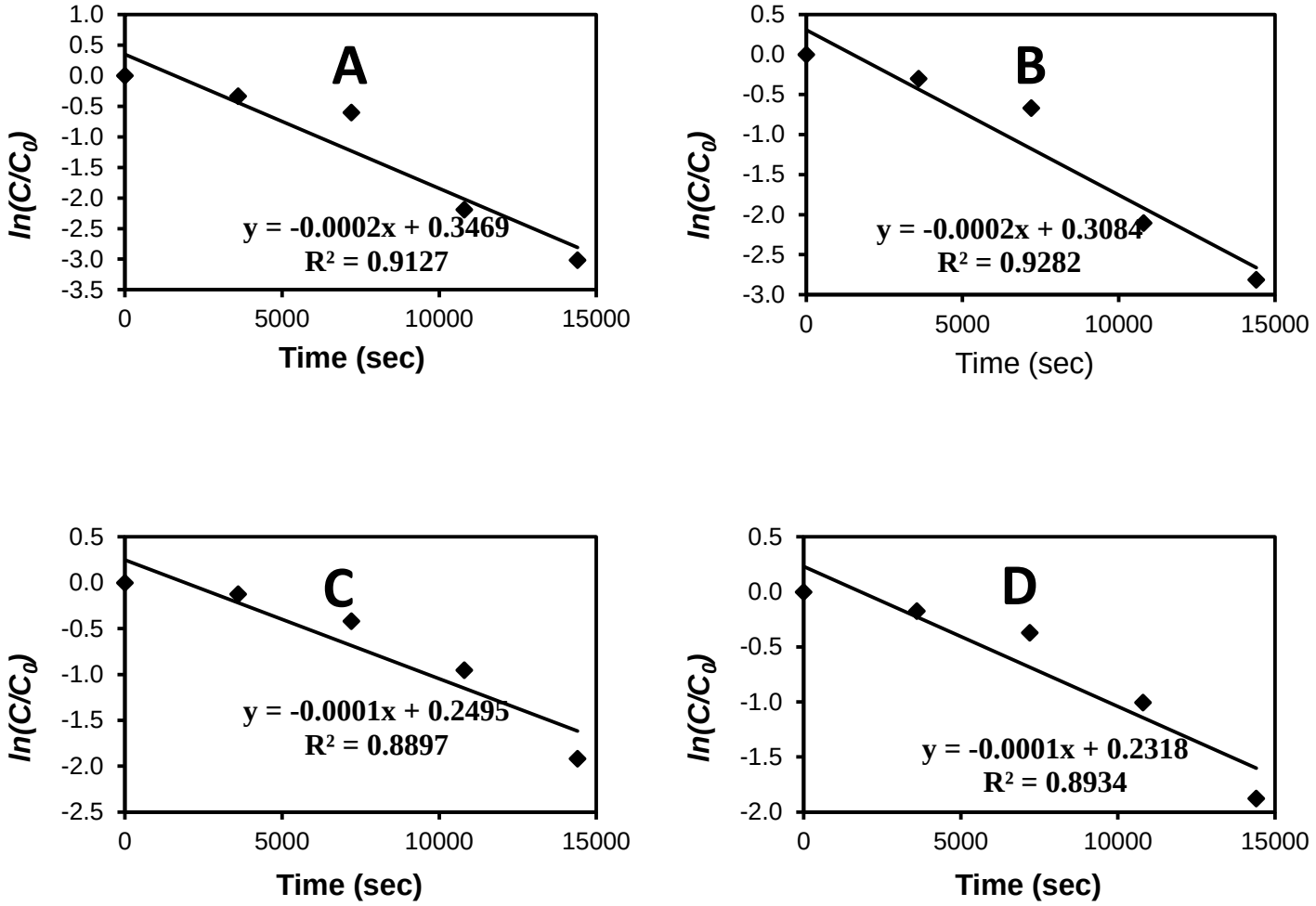

Figure 23. Kinetic plots of (A) NiMo/AC (B) NiMo/AC200, (C) NiMo/AC300 and (D) NiMo/AC400

4.2.3 Effects of ultrasonication and Chelating agents

The results of the HDS activity tests for each all materials are presented in Table 10. Analysis of the results shows that the catalyst there is a significant difference in the performance of the catalyst towards the HDS of DBT, Figure 24. Starting with the NiMo series, it is evident that NiMo/AC(EDTA) each catalyst the most effective of the three catalysts. The concentration of sulfur is reduced by to less than 10ppm for the reaction involving NiMo/AC(EDTA) while the concentration of sulfur in aliquots obtained at the same time interval using NiMo/AC(CA) or NiMo/AC(U-S) was above 50ppm. Comparison of the sulfur concentration in aliquots from reactions involving NiMo/AC(CA) and NiMo/AC(U-S) reveals that more DBT HDS was achieved when catalysts were prepared using citric acid to enhance dispersion rather ultrasonication. Further analysis of the results showed that a similar pattern of performance observed with the CoMo/AC series but the concentration of sulfur in the aliquots are much lower compared to the NiMo/AC. An obvious example is the concentration of sulfur in aliquots taken from the reactor after the third hour. As for CoMo/AC(CA), the concentration of sulfur was reduced to the below detectable limit while the concentration was above 5ppm in the case of the reactions involving NiMo/AC(EDTA). The observed trend is an indication that EDTA was more effective in the dispersion of the active phased compared to ultrasonication and even citric acid.

Table 10. HDS Test Results: Performance of MAC, NMAC and CMAC catalysts

Catalysts	Concentration of DBT in products taken at intervals (ppm)			
	Set point (0h)	1h	2h	3h
NiMo/AC(U-S)	520	359	305	78
NiMo/AC(CA)	703	377	166	75
NiMo/AC(EDTA)	634	364	141	36

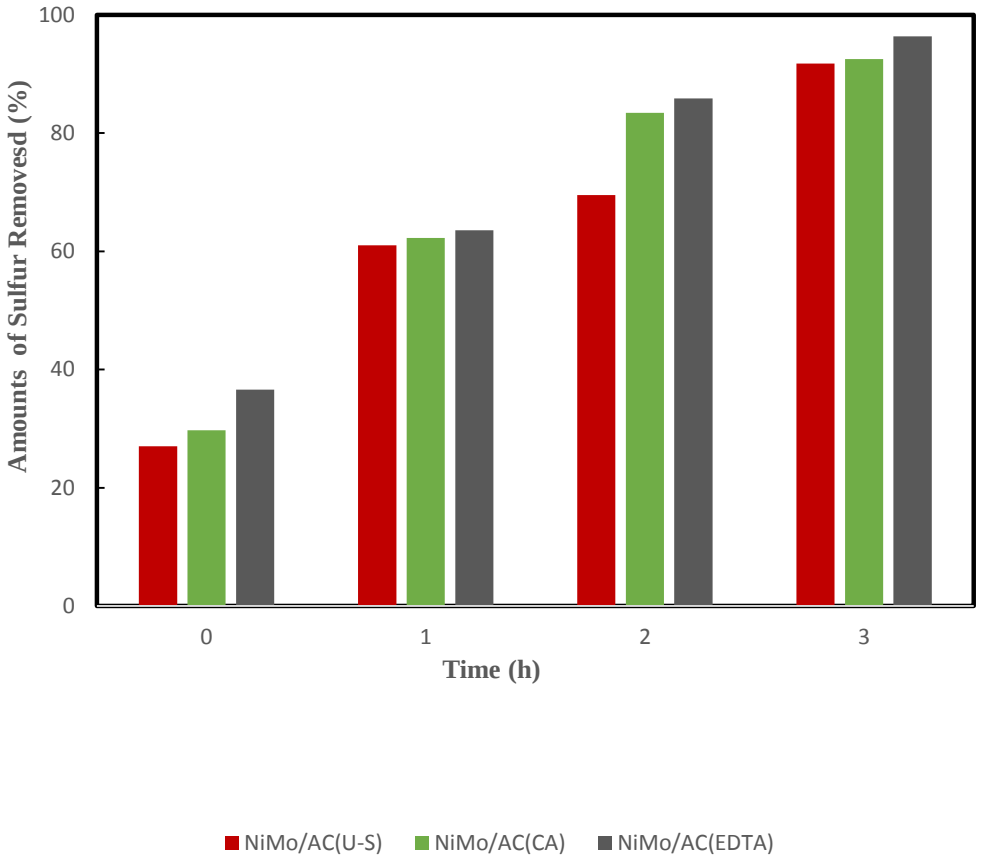

Figure 24. Amounts of sulfur removed using NiMo/AC(U-S), NiMo/AC(CA) and NiMo/AC(EDTA)

Results for the kinetics study of NiMo/AC(U-S), NiMo/AC(CA) and NiMo/AC(EDTA) are presented in Table 11. HDS rate constants k (s^{-1}), $ks^{-1}g^{-1}$cat. and R^2 values were calculated for the three catalysts. The magnitude of the R^2 values range from 0.850 to 0.989, an indication that the reactions involving all the tested catalysts agree well with the proposed pseudo-first order kinetics for the desulfurization process using supported Mo catalysts. Calculations for the nth order rates yielded lower R^2 values. The results also show a strong correlation between the performance of the catalysts towards the desulfurization of DBT and the magnitude of the pseudo 1^{st} order rate constants. For example, the HDS rate constant for NiMo/AC(EDTA), NiMo/AC(CA), NiMo/AC(U-S) and NiMo/AC are is 2.3×10^{-4} s^{-1}, 1.8×10^{-4} s^{-1}, 1.6×10^{-4} s^{-1} and 1.5×10^{-4} s^{-1} respectively, Figure 25. The differences in the magnitude of the HDS rate constants reflect the relative performance of the catalysts and, therefore, provides more insight into the activity of the prepared catalysts. It is now clear that NiMo/AC(EDTA) is most effective of the prepared and tested catalysts in the degradation of DBT. The magnitude of the HDS rates constants also indicates that the chelating agents are more effective in the dispersion of active metal species when compared to ultrasonication.

Table 11. Kinetic parameters: HDS Rate constants for NiMo/AC(U-S), NiMo/AC(CA) and NiMo/AC(EDTA)

Catalysts	1st Order Kinetics Constants			
	k_{HDS} (s^{-1})	$k_{HDS}\times10^{4}$ (s^{-1})	$k_{HDS}\times10^{4}$ ($s^{-1}g^{-1}cat$)	R^2
NiMo/AC(U-S)	1.6E-04	1.6E+00	5.22	0.921
NiMo/AC(CA)	1.8E-04	1.84	6.15	0.850
NiMo/AC(EDTA)	2.3E-04	2.26	7.53	0.981

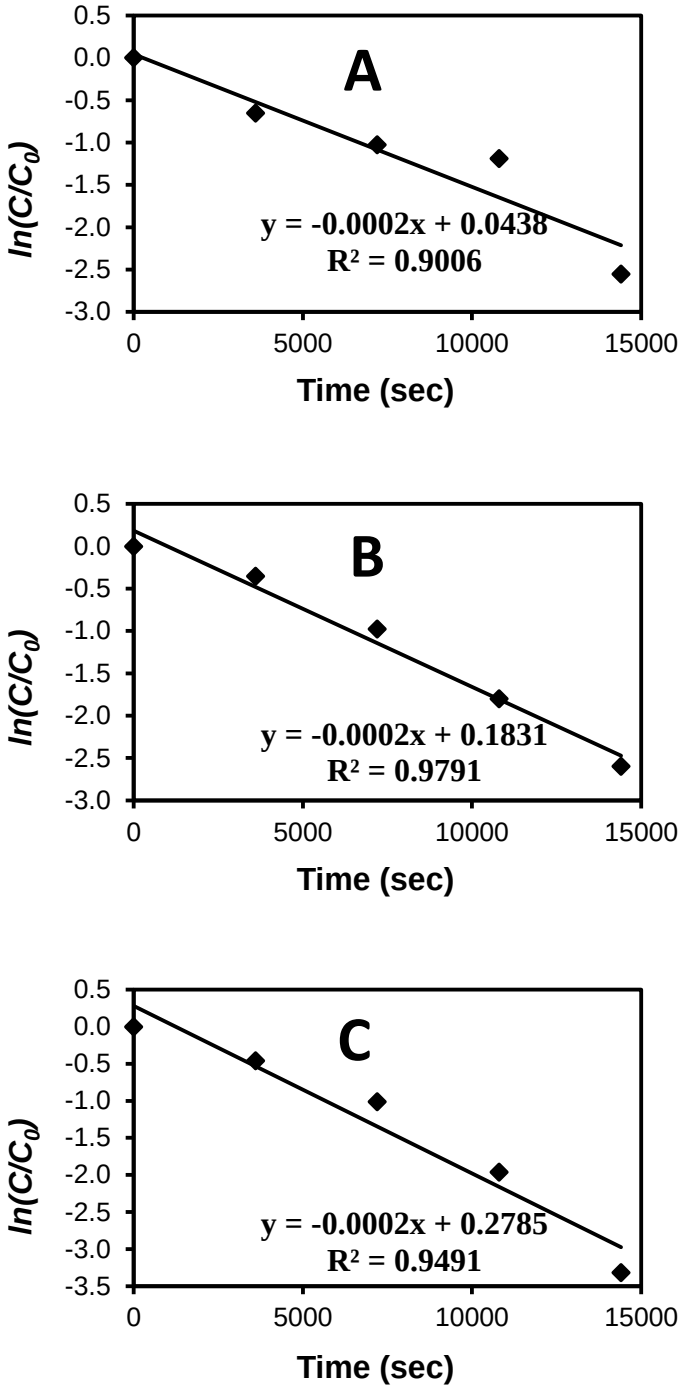

Figure 25. Kinetic plots of NiMo/AC(U-S), (B) NiMo/AC(CA) and (C) NiMo/AC(EDTA)

CHAPTER 5

Conclusion and Recommendation

5.1 Conclusions

A set of Mo based catalysts supported on activated carbon derived from waste tires, TiO_2 and AC-TiO_2 composites supports were prepared and applied in the HDS of DBT. The catalysts were characterized by various techniques including N_2-physisorption, X-ray diffraction (XRD) and FTIR. The HDS activity of the catalyst was tested in a pressure batch reactor using decalin spiked with dibenzothiophene as model fuel. The activity of the catalyst was found to be dependent on the composition of the catalysts and support material as well as the preparation methods.

The activated carbon support was found to be the most effective for the catalysts when compared with TiO_2 and the AC-TIO_2 composite supports. Results from the characterization and the catalytic activity tests show that the chelating agents were more effective in the dispersion of the active phase and the HDS activity was highest activity was observed when EDTA was used.

Direct desulfurization was identified and most favored reaction route and higher desulfurization of the DBT was achieved in a shorter time with the NiMo/AC, especially when EDTA was used to aid the dispersion of the active phase.

5.2 Recommendations

More studies should be conducted to compare the effectiveness of the activated carbon from the waste tire with other activated carbon materials with the larger surface area and other distinct textural characteristics.

More metal oxides and activated carbon-metal oxide composites should be should be prepared and tested. Different preparation methods for the metal oxide and the activated carbon-metal oxide could be adopted to improve for improved performance.

The investigation should be extended to adsorptive desulfurization to ascertain the extent of the effect of calcination on the performance of molybdenum and other active species supported on carbon materials.

APPENDIX

Example of the GC-MS chromatogram obtained of the products of HDS using the prepared catalyst NiMo-AC300

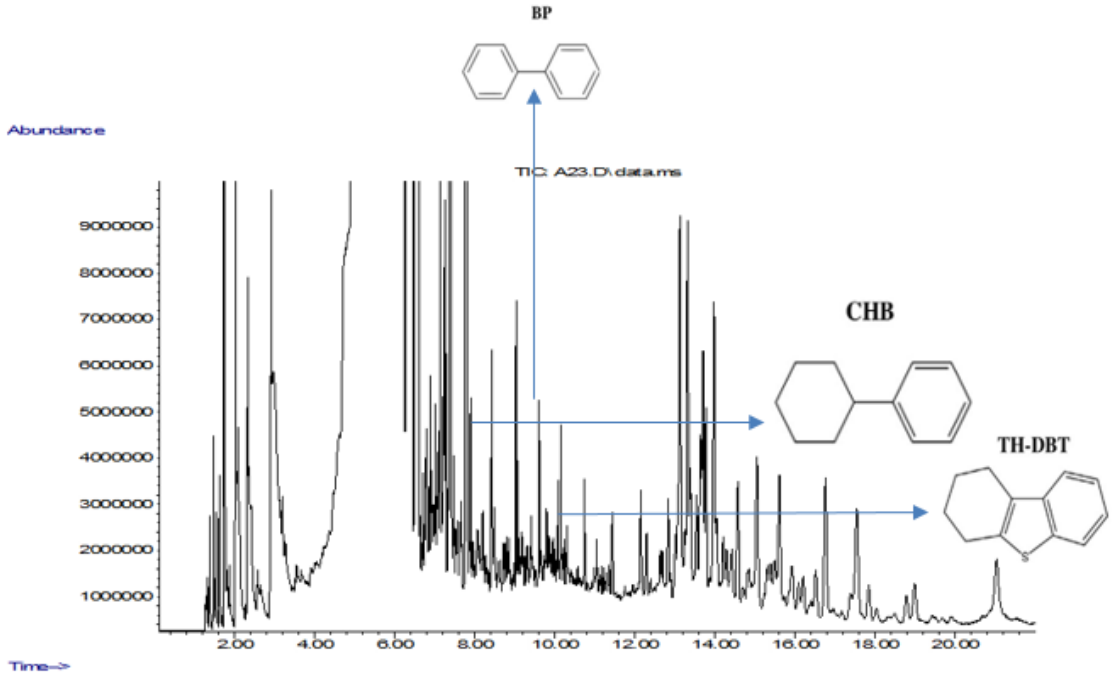

Example of the GC-MS chromatogram obtained of the products of HDS using the prepared catalyst NiMo-AC400

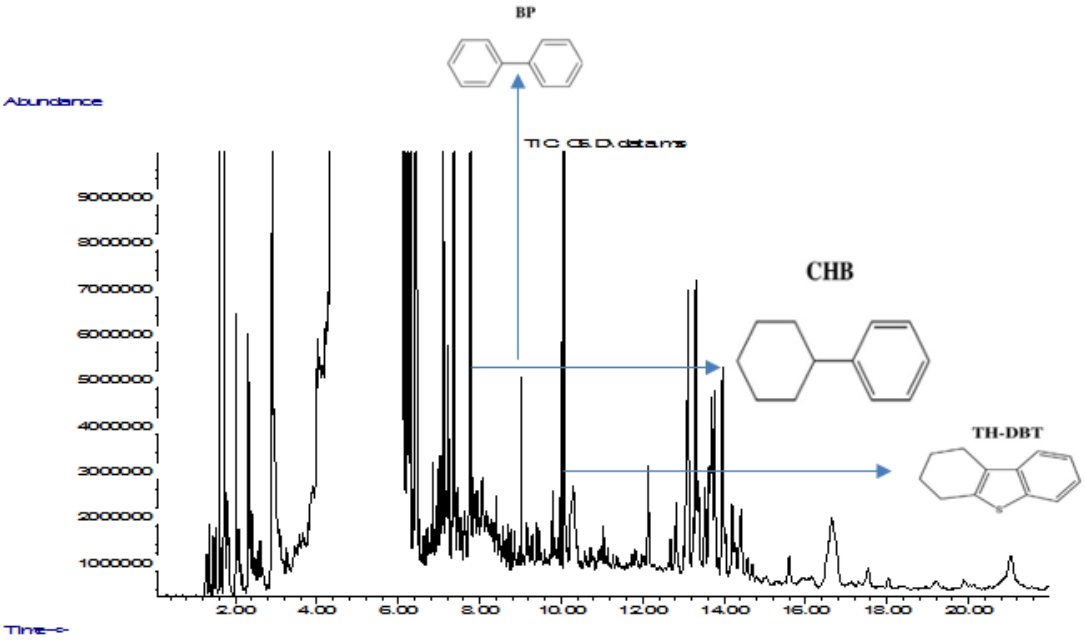

References

[1] Y. Wang, F. H. Yang, R. T. Yang, J. M. Heinzel, and A. D. Nickens, "Desulfurization of high-sulfur jet fuel by π-complexation with copper and palladium halide sorbents," *Ind. Eng. Chem. Res.*, vol. 45, no. 22, pp. 7649–7655, 2006.

[2] C. Song, "An overview of new approaches to deep desulfurization for ultra-clean gasoline, diesel fuel and jet fuel," *Catal. Today*, vol. 86, no. 1–4, pp. 211–263, 2003.

[3] W. Li, J. Liu, and D. Zhao, "Mesoporous materials for energy conversion and storage devices," *Nat. Rev. Mater.*, vol. 1, no. 6, p. 16023, 2016.

[4] S. Ma, L. Gao, J. Ma, X. Jin, J. Yao, and Y. Zhao, "Advances on simultaneous desulfurization and denitrification using activated carbon irradiated by microwaves," *Environ. Technol.*, vol. 33, no. 11, pp. 1225–1230, 2012.

[5] A. H. M. S. Hussain and B. J. Tatarchuk, "Adsorptive desulfurization of jet and diesel fuels using Ag/TiOx–Al 2 O 3 and Ag/TiOx–SiO 2 adsorbents," *Fuel*, vol. 107, no. 0, pp. 465–473, 2013.

[6] S. A. Ganiyu, S. A. Ali, and K. Alhooshani, "Simultaneous HDS of DBT and 4,6-DMDBT over single-pot Ti-SBA-15-NiMo catalysts: influence of Si/Ti ratio on the structural properties, dispersion and catalytic activity," *RSC Adv.*, vol. 7, no. 35, pp. 21943–21952, 2017.

[7] S. Nair and B. J. Tatarchuk, "Supported silver adsorbents for selective removal of

sulfur species from hydrocarbon fuels," *Fuel*, vol. 89, no. 11, pp. 3218–3225, 2010.

[8] R. T. Yang, *Fundamentals and applications*. 2001.

[9] T. A. Saleh and G. I. Danmaliki, "Influence of acidic and basic treatments of activated carbon derived from waste rubber tires on adsorptive desulfurization of thiophenes," *J. Taiwan Inst. Chem. Eng.*, vol. 60, pp. 460–468, 2016.

[10] A. H. M. S. Hussain and B. J. Tatarchuk, "Adsorptive desulfurization of jet and diesel fuels using Ag/TiO x-Al2O3 and Ag/TiOx-SiO2 adsorbents," *Fuel*, vol. 107, pp. 465–473, 2013.

[11] M. Teymouri, A. Samadi-Maybodi, A. Vahid, and A. Miranbeigi, "Adsorptive desulfurization of low sulfur diesel fuel using palladium containing mesoporous silica synthesized via a novel in-situ approach," *Fuel Process. Technol.*, vol. 116, 2013.

[12] I. Ahmed and S. H. Jhung, "Adsorptive desulfurization and denitrogenation using metal-organic frameworks," *Journal of Hazardous Materials*, vol. 301. pp. 259–276, 2016.

[13] M. V Landau, L. Vradman, M. Herskowitz, Y. Koltypin, and A. Gedanken, "Ultrasonically Controlled Deposition-Precipitation Co-Mo HDS Catalysts Deposited on Wide-Pore MCM Material," *J. Catal.*, vol. 201, pp. 22–36, 2005.

[14] Y. V. Joshi, P. Ghosh, M. Daage, and W. N. Delgass, "Support effects in HDS catalysts: DFT analysis of thiolysis and hydrolysis energies of metal-support linkages," *J. Catal.*, vol. 257, no. 1, pp. 71–80, 2008.

[15] I. Ahmed, Z. Hasan, N. A. Khan, and S. H. Jhung, "Adsorptive denitrogenation of model fuels with porous metal-organic frameworks (MOFs): Effect of acidity and basicity of MOFs," *Appl. Catal. B Environ.*, vol. 129, pp. 123–129, 2013.

[16] P. A. Nikulshin, N. N. Tomina, A. A. Pimerzin, A. V. Kucherov, and V. M. Kogan, "Investigation into the effect of the intermediate carbon carrier on the catalytic activity of the HDS catalysts prepared using heteropolycompounds," *Catal. Today*, vol. 149, no. 1–2, pp. 82–90, 2010.

[17] P. A. Nikulshin, V. A. Salnikov, A. V. Mozhaev, P. P. Minaev, V. M. Kogan, and A. A. Pimerzin, "Relationship between active phase morphology and catalytic properties of the carbon-alumina-supported Co(Ni)Mo catalysts in HDS and HYD reactions," *J. Catal.*, vol. 309, pp. 386–396, 2014.

[18] J. J. Lee, S. Han, H. Kim, J. H. Koh, T. Hyeon, and S. H. Moon, "Performance of CoMoS catalysts supported on nanoporous carbon in the hydrodesulfurization of dibenzothiophene and 4,6-dimethyldibenzothiophene," *Catal. Today*, vol. 86, no. 1–4, pp. 141–149, 2003.

[19] S. Brunet, D. Mey, G. P??rot, C. Bouchy, and F. Diehl, "On the hydrodesulfurization of FCC gasoline: A review," *Applied Catalysis A: General*, vol. 278, no. 2. pp. 143–172, 2005.

[20] D. D. Link and P. Zandhuis, "The distribution of sulfur compounds in hydrotreated jet fuels: Implications for obtaining low-sulfur petroleum fractions," *Fuel*, vol. 85, no. 4. pp. 451–455, 2006.

[21] T. P. Silva, S. M. Paixão, A. V. Teixeira, J. C. Roseiro, and L. Alves, "Optimization of low sulfur carob pulp liquor as carbon source for fossil fuels biodesulfurization," *J. Chem. Technol. Biotechnol.*, vol. 88, no. 5, pp. 919–923, 2013.

[22] D. Montalván-Sorrosa, D. De Los Cobos-Vasconcelos, and A. González-Sánchez, "Nanotechnology Applied to the Biodesulfurization of Fossil Fuels and Spent Caustic Streams," in *Applying Nanotechnology to the Desulfurization Process in Petroleum Engineering*, 2016, pp. 378–389.

[23] L. He, H. Li, W. Zhu, J. Guo, X. Jiang, J. Lu, and Y. Yan, "Deep oxidative desulfurization of fuels using peroxophosphomolybdate catalysts in ionic liquids," *Ind. Eng. Chem. Res.*, vol. 47, no. 18, pp. 6890–6895, 2008.

[24] W. Zhu, Y. Ding, H. Li, J. Qin, Y. Chao, J. Xiong, Y. Xu, and H. Liu, "Application of a self-emulsifiable task-specific ionic liquid in oxidative desulfurization of fuels.," *RSC Adv.*, vol. 3, no. 12, pp. 3893–3898, 2013.

[25] W. Jiang, W. Zhu, Y. Chang, Y. Chao, S. Yin, H. Liu, F. Zhu, and H. Li, "Ionic liquid extraction and catalytic oxidative desulfurization of fuels using dialkylpiperidinium tetrachloroferrates catalysts," *Chem. Eng. J.*, vol. 250, pp. 48–54, 2014.

[26] F. Li, Y. Liu, Z. Sun, Y. Zhao, R. Liu, L. Chen, and D. Zhao, "Photocatalytic oxidative desulfurization of dibenzothiophene under simulated sunlight irradiation with mixed-phase Fe2O3 prepared by solution combustion," *Catal. Sci. Technol.*, vol. 2, no. 7, p. 1455, 2012.

[27] T. H. T. Vu, T. T. T. Nguyen, P. H. T. Nguyen, M. H. Do, H. T. Au, T. B. Nguyen, D. L. Nguyen, and J. S. Park, "Fabrication of photocatalytic composite of multi-walled carbon nanotubes/TiO 2 and its application for desulfurization of diesel," *Mater. Res. Bull.*, vol. 47, no. 2, pp. 308–314, 2012.

[28] M. Zarrabi and M. H. Entezari, "Modification of C/TiO2@MCM-41 with nickel nanoparticles for photocatalytic desulfurization enhancement of a diesel fuel model under visible light.," *J. Colloid Interface Sci.*, vol. 457, pp. 353–9, 2015.

[29] J. Wang, F. Xu, W. jie Xie, Z. jian Mei, Q. zhuo Zhang, J. Cai, and W. min Cai, "The enhanced adsorption of dibenzothiophene onto cerium/nickel-exchanged zeolite Y," *J. Hazard. Mater.*, vol. 163, no. 2–3, pp. 538–543, 2009.

[30] H. Song, X. Cui, H. Gao, and F. Li, "Characteristic and Adsorption Desulfurization Performance of Ag–Ce Bimetal Ion-Exchanged Y Zeolite," *Ind. Eng. Chem. Res.*, vol. 53, no. 37, pp. 14552–14557, 2014.

[31] N. A. Khan and S. H. Jhung, "Scandium-Triflate/Metal-Organic Frameworks: Remarkable Adsorbents for Desulfurization and Denitrogenation," *Inorg. Chem.*, vol. 54, no. 23, pp. 11498–11504, 2015.

[32] H. Song, Y. Chang, and H. Song, "Deep adsorptive desulfurization over Cu, Ce bimetal ion-exchanged Y-typed molecule sieve," *Adsorption*, vol. 22, no. 2, pp. 139–150, 2016.

[33] R. Abro, A. a Abdeltawab, S. S. Al-deyab, G. Yu, A. B. Qazi, S. Gao, and X. Chen, "RSC Advances A review of extractive desulfurization of fuel oils," *RSC Adv.*, vol.

4, pp. 35302–35317, 2014.

[34] J. M. Campos-Martin, M. C. Capel-Sanchez, P. Perez-Presas, and J. L. G. Fierro, "Oxidative processes of desulfurization of liquid fuels," *Journal of Chemical Technology and Biotechnology*, vol. 85, no. 7. pp. 879–890, 2010.

[35] Z. Ismagilov, S. Yashnik, M. Kerzhentsev, V. Parmon, a. Bourane, F. M. Al-Shahrani, a. a. Hajji, and O. R. Koseoglu, "Oxidative Desulfurization of Hydrocarbon Fuels," *Catal. Rev.*, vol. 53, no. 3, pp. 199–255, 2011.

[36] A. W. Bhutto, R. Abro, S. Gao, T. Abbas, X. Chen, and G. Yu, "Oxidative desulfurization of fuel oils using ionic liquids: A review," *J. Taiwan Inst. Chem. Eng.*, vol. 62, pp. 84–97, 2016.

[37] G. Mohebali and A. S. Ball, "Biodesulfurization of diesel fuels - Past, present and future perspectives," *International Biodeterioration and Biodegradation*, vol. 110. pp. 163–180, 2016.

[38] Y. Zhang, Y. Yang, H. Han, M. Yang, L. Wang, Y. Zhang, Z. Jiang, and C. Li, "Ultra-deep desulfurization via reactive adsorption on Ni/ZnO: The effect of ZnO particle size on the adsorption performance," *Appl. Catal. B Environ.*, vol. 119–120, pp. 13–19, 2012.

[39] R. Ullah, P. Bai, P. Wu, Z. Zhang, Z. Zhong, U. J. Etim, F. Subhan, and Z. Yan, "Comparison of the Reactive Adsorption Desulfurization Performance of Ni/ZnO–Al 2 O 3 Adsorbents Prepared by Different Methods," *Energy & Fuels*, vol. 30, no. 4, pp. 2874–2881, Apr. 2016.

[40] C. Song and X. Ma, “New design approaches to ultra-clean diesel fuels by deep desulfurization and deep dearomatization,” in *Applied Catalysis B: Environmental*, 2003, vol. 41, no. 1–2, pp. 207–238.

[41] R. T. Yang, *Adsorbents Adsorbents : Fundamentals and Applications*. 2003.

[42] F. Rezaei and P. Webley, “Structured adsorbents in gas separation processes,” *Separation and Purification Technology*, vol. 70, no. 3. pp. 243–256, 2010.

[43] Y. Zhao, X. Liu, and Y. Han, “Microporous carbonaceous adsorbents for CO2 separation via selective adsorption,” *RSC Adv.*, vol. 5, no. 38, pp. 30310–30330, 2015.

[44] A. Bhatnagar, W. Hogland, M. Marques, and M. Sillanpää, “An overview of the modification methods of activated carbon for its water treatment applications,” *Chem. Eng. J.*, vol. 219, pp. 499–511, 2013.

[45] M. J. K. Ahmed and M. Ahmaruzzaman, “Adsorptive desulfurization of feed diesel using chemically impregnated coconut coir waste,” *Int. J. Environ. Sci. Technol.*, vol. 12, no. 9, pp. 2847–2856, 2015.

[46] T. A. Saleh and G. I. Danmaliki, “Adsorptive desulfurization of dibenzothiophene from fuels by rubber tyres-derived carbons: Kinetics and isotherms evaluation,” *Process Saf. Environ. Prot.*, vol. 102, pp. 9–19, 2016.

[47] A. R. Lopes, A. de P. Scheer, G. V. Silva, and C. I. Yamamoto, “Pd-Impregnated activated carbon and treatment acid to remove sulfur and nitrogen from diesel,” *Rev. Mater.*, vol. 21, no. 2, pp. 407–415, 2016.

[48] C. Moreno-Castilla, F. Carrasco-Marín, and A. Mueden, "The Creation of Acid Carbon Surfaces by Treatment with (NH4)2S2O8," *Carbon N. Y.*, vol. 35, no. 10–11, pp. 1619–1626, 1997.

[49] M. V. Lopez-Ramon, F. Stoeckli, C. Moreno-Castilla, and F. Carrasco-Marin, "On the characterization of acidic and basic surface sites on carbons by various techniques," *Carbon N. Y.*, vol. 37, no. 8, pp. 1215–1221, 1999.

[50] C. Moreno-Castilla, M. . López-Ramón, F. Carrasco-Marín, M. V Lopez-Ramon, and F. Carrasco-Marin, "Changes in surface chemistry of activated carbons by wet oxidation," *Carbon N. Y.*, vol. 38, no. 14, pp. 1995–2001, 2000.

[51] V. Selvavathi, V. Chidambaram, A. Meenakshisundaram, B. Sairam, and B. Sivasankar, "Adsorptive desulfurization of diesel on activated carbon and nickel supported systems," *Catal. Today*, vol. 141, no. 1–2, pp. 99–102, 2009.

[52] L. S. Ferreira and J. O. Trierweiler, "Modeling and simulation of the polymeric nanocapsule formation process," *IFAC Proc. Vol.*, vol. 7, no. PART 1, pp. 405–410, 2009.

[53] S. P. Hernandez, D. Fino, and N. Russo, "High performance sorbents for diesel oil desulfurization," *Chem. Eng. Sci.*, vol. 65, no. 1, pp. 603–609, 2010.

[54] J.-X. Guo, Y.-F. Qu, S. Shu, X.-J. Wang, H.-Q. Yin, and Y.-H. Chu, "Effects of preparation conditions on Mn-based activated carbon catalysts for desulfurization," *New J. Chem.*, vol. 39, no. x, pp. 5997–6015, 2015.

[55] H. P. Ho, P. Kasinathan, J. Kim, D. Lee, and H. C. Woo, "Deep desulfurization of

fuel gas by adsorption on Cu-impregnated activated carbons in practical conditions," *Korean J. Chem. Eng.*, vol. 33, no. 6, pp. 1908–1916, 2016.

[56] S. K. Thaligari, S. Gupta, V. C. Srivastava, and B. Prasad, "Simultaneous Desulfurization and Denitrogenation of Liquid Fuel By Nickel Modified Granular Activated Carbon," *Energy & Fuels*, p. acs.energyfuels.6b00579, 2016.

[57] H. Cui, S. Q. Turn, and M. a Reese, "Adsorptive Removal of Tetrahydrothiophene (THT) from Synthetic Natural Gas on Modified Activated Carbons," *Energy*, vol. 5, no. 4, pp. 2550–2558, 2008.

[58] Y. Wang and R. T. Yang, "Desulfurization of liquid fuels by adsorption on carbon-based sorbents and ultrasound-assisted sorbent regeneration," *Langmuir*, vol. 23, no. 7, pp. 3825–3831, 2007.

[59] M. Balsamo, S. Cimino, G. de Falco, A. Erto, and L. Lisi, "ZnO-CuO supported on activated carbon for H2S removal at room temperature," *Chem. Eng. J.*, vol. 304, pp. 399–407, 2016.

[60] G. I. Danmaliki and T. A. Saleh, "Effects of bimetallic Fe−Ce nanoparticles on the desulfurization of thiophenes using activated carbon," *Chem. Eng. J.*, Aug. 2016.

[61] B. N. Bhadra, K. H. Cho, N. A. Khan, D. Y. Hong, and S. H. Jhung, "Liquid-Phase Adsorption of Aromatics over a Metal-Organic Framework and Activated Carbon: Effects of Hydrophobicity/Hydrophilicity of Adsorbents and Solvent Polarity," *J. Phys. Chem. C*, vol. 119, no. 47, pp. 26620–26627, 2015.

[62] C. J. Rhodes, "Properties and applications of zeolites," *Sci. Prog.*, vol. 93, no. 3, pp.

223–284, 2010.

[63] S. Velu, X. Ma, and C. Song, “Selective Adsorption for Removing Sulfur from Jet Fuel over Zeolite-Based Adsorbents,” *Ind. Eng. Chem. Res.*, vol. 42, no. 21, pp. 5293–5304, 2003.

[64] R. Mahmoudi and C. Falamaki, “Ni2+-ion-exchanged dealuminated clinoptilolite: A superior adsorbent for deep desulfurization,” *Fuel*, vol. 173, pp. 277–284, 2016.

[65] A. Takahashi, F. H. Yang, and R. T. Yang, “New Sorbents for Desulfurization by π-Complexation: Thiophene/Benzene Adsorption,” *Ind. Eng. Chem. Res.*, vol. 41, no. 10, pp. 2487–2496, 2002.

[66] H. Song, H. Song, X. Wan, M. Dai, J. Zhang, and F. Li, “Deep desulfurization of model gasoline by selective adsorption over Cu-Ce bimetal ion-exchanged y zeolite,” *Fuel Process. Technol.*, vol. 116, pp. 52–62, 2013.

[67] M. Alhamami, H. Doan, and C. H. Cheng, “A review on breathing behaviors of metal-organic-frameworks (MOFs) for gas adsorption,” *Materials*, vol. 7, no. 4. pp. 3198–3250, 2014.

[68] N. A. Khan, Z. Hasan, and S. H. Jhung, “Adsorptive removal of hazardous materials using metal-organic frameworks (MOFs): A review,” *Journal of Hazardous Materials*, vol. 244–245. pp. 444–456, 2013.

[69] X. Liu, J. Wang, Q. Li, S. Jiang, T. Zhang, and S. Ji, “Synthesis of rare earth metal-organic frameworks (Ln-MOFs) and their properties of adsorption desulfurization,” *J. Rare Earths*, vol. 32, no. 2, pp. 189–194, 2014.

[70] P. Falcaro, R. Ricco, A. Yazdi, I. Imaz, S. Furukawa, D. Maspoch, R. Ameloot, J. D. Evans, and C. J. Doonan, "Application of metal and metal oxide nanoparticles@MOFs," *Coord. Chem. Rev.*, vol. 307, Part, pp. 237–254, 2016.

[71] M. Kim, J. F. Cahill, H. Fei, K. A. Prather, and S. M. Cohen, "Postsynthetic Ligand and Cation Exchange in Robust Metal-Organic Frameworks," *J. Am. Chem. Soc.*, vol. 134, no. 43, pp. 18082–18088, 2012.

[72] Z. Fang, B. Bueken, D. E. De Vos, and R. A. Fischer, "Defect-Engineered Metal-Organic Frameworks," *Angew. Chemie - Int. Ed.*, vol. 54, no. 25, pp. 7234–7254, 2015.

[73] B. Gui, X. Meng, H. Xu, and C. Wang, "Postsynthetic Modification of Metal-Organic Frameworks through Click Chemistry," *Chinese Journal of Chemistry*, vol. 34, no. 2. pp. 186–190, 2016.

[74] D. Zacher, R. Schmid, C. Wöll, and R. A. Fischer, "Surface chemistry of metal-organic frameworks at the liquid-solid interface," *Angewandte Chemie - International Edition*, vol. 50, no. 1. pp. 176–199, 2011.

[75] B. Van de Voorde, B. Bueken, J. Denayer, and D. De Vos, "Adsorptive separation on metal-organic frameworks in the liquid phase.," *Chem. Soc. Rev.*, vol. 43, no. 16, pp. 5766–88, 2014.

[76] K. a. Cychosz, A. G. Wong-Foy, and A. J. Matzger, "Liquid Phase Adsorption by Microporous Coordination\rPolymers: Removal of Organosulfur Compounds," *J. Am. Chem. Soc.*, vol. 130, no. 22, pp. 6938–6939, 2008.

[77] N. A. Khan and S. H. Jhung, “Low-temperature loading of Cu+ species over porous metal-organic frameworks (MOFs) and adsorptive desulfurization with Cu+-loaded MOFs,” *J. Hazard. Mater.*, vol. 237–238, pp. 180–185, 2012.

[78] N. A. Khan, J. W. Jun, J. H. Jeong, and S. H. Jhung, “Remarkable adsorptive performance of a metal-organic framework, vanadium-benzenedicarboxylate (MIL-47), for benzothiophene.,” *Chem. Commun. (Camb).*, vol. 47, no. 4, pp. 1306–1308, 2011.

[79] Y. X. Li, W. J. Jiang, P. Tan, X. Q. Liu, D. Y. Zhang, and L. B. Sun, “What matters to the adsorptive desulfurization performance of metal - Organic frameworks?,” *J. Phys. Chem. C*, vol. 119, no. 38, pp. 21969–21977, 2015.

[80] N. A. Khan, Z. Hasan, and S. H. Jhung, “Ionic liquids supported on metal-organic frameworks: Remarkable adsorbents for adsorptive desulfurization,” *Chem. - A Eur. J.*, vol. 20, no. 2, pp. 376–380, 2014.

[81] J.-X. Qin, P. Tan, Y. Jiang, X.-Q. Liu, Q.-X. He, and L.-B. Sun, “Functionalization of metal–organic frameworks with cuprous sites using vapor-induced selective reduction: efficient adsorbents for deep desulfurization,” *Green Chem.*, vol. 15, no. 2, pp. 439–445, 2016.

[82] N. A. Khan, Z. Hasan, and S. H. Jhung, “Ionic liquid@MIL-101 prepared via the ship-in-bottle technique: Remarkable adsorbents for the removal of benzothiophene from liquid fuel,” *Chem. Commun.*, vol. 52, no. 12, pp. 2561–2564, 2016.

[83] J. Juan-Alcaniz, J. Gascon, and F. Kapteijn, “Metal-organic frameworks as scaffolds

for the encapsulation of active species: state of the art and future perspectives," *J. Mater. Chem.*, vol. 22, no. 20, pp. 10102–10118, 2012.

[84] D. Wu, F. Xu, B. Sun, R. Fu, H. He, and K. Matyjaszewski, "Design and preparation of porous polymers.," *Chem. Rev.*, vol. 112, no. 7, pp. 3959–4015, Jul. 2012.

[85] B. Li, Y. Zhang, D. Ma, Z. Shi, and S. Ma, "Mercury nano-trap for effective and efficient removal of mercury(II) from aqueous solution.," *Nat. Commun.*, vol. 5, no. May, p. 5537, 2014.

[86] T. Jin, S. An, X. Yang, J. Hu, H. Wang, H. Liu, Z. Tian, D. Jiang, N. Mehio, and X. Zhu, "Efficient adsorptive desulfurization by task-specific porous organic polymers," *AIChE J.*, vol. 62, no. 5, pp. 1740–1746, May 2016.

[87] X. Sun and B. J. Tatarchuk, "Photo-assisted adsorptive desulfurization of hydrocarbon fuels over TiO2 and Ag/TiO2," *Fuel*, vol. 183, pp. 550–556, 2016.

[88] J. Xiao, S. Sitamraju, Y. Chen, S. Watanabe, M. Fujii, M. Janik, and C. Song, "Air-promoted adsorptive desulfurization of diesel fuel over Ti-Ce mixed metal oxides," *AIChE J.*, vol. 61, no. 2, pp. 631–639, 2015.

[89] H. Faghihian and R. Sadeghinia, "Photo Degradation-Adsorption Process as a Novel Desulfurization Method," *Adv. Chem. Eng. Res.*, vol. 3, no. 3, 2014.

[90] S. Moradi, M. Vossoughi, M. Feilizadeh, S. M. E. Zakeri, M. M. Mohammadi, D. Rashtchian, and A. Yoosefi Booshehri, "Photocatalytic degradation of dibenzothiophene using La/PEG-modified TiO2 under visible light irradiation," *Res. Chem. Intermed.*, pp. 4151–4167, 2014.

[91] M. Zarrabi, M. H. Entezari, and E. K. Goharshadi, “Photocatalytic oxidative desulfurization of dibenzothiophene by C/TiO $_2$ @MCM-41 nanoparticles under visible light and mild conditions,” *RSC Adv.*, vol. 5, no. 44, pp. 34652–34662, 2015.

[92] W. Lei, W. Wenya, N. Mominou, L. Liu, and S. Li, “Ultra-deep desulfurization of gasoline through aqueous phase in-situ hydrogenation and photocatalytic oxidation,” *Appl. Catal. B Environ.*, vol. 193, pp. 180–188, 2016.

[93] B. M. Reddy and A. Khan, “Recent Advances on TiO $_2$ -ZrO $_2$ Mixed Oxides as Catalysts and Catalyst Supports,” *Catal. Rev.*, vol. 47, no. 2, pp. 257–296, Apr. 2005.

[94] Z. Xie, Z. Liu, Y. Wang, Q. Yang, L. Xu, and W. Ding, “An overview of recent development in composite catalysts from porous materials for various reactions and processes.,” *Int. J. Mol. Sci.*, vol. 11, no. 5, pp. 2152–87, May 2010.

[95] J. M. Badano, C. Betti, I. Rintoul, J. Vich-Berlanga, E. Cagnola, G. Torres, C. Vera, J. Yori, and M. Quiroga, “New composite materials as support for selective hydrogenation; egg-shell catalysts,” *Appl. Catal. A Gen.*, vol. 390, no. 1–2, pp. 166–174, Dec. 2010.

[96] Y. Deng, Y. Cai, Z. Sun, J. Liu, C. Liu, J. Wei, W. Li, C. Liu, Y. Wang, and D. Zhao, “Multifunctional Mesoporous Composite Microspheres with Well-Designed Nanostructure: A Highly Integrated Catalyst System,” *J. Am. Chem. Soc.*, vol. 132, no. 24, pp. 8466–8473, Jun. 2010.

[97] E. A. Belopukhov and A. S. Belyi, “Mechanical Strength of Composite Supports for

Catalysts Based on γ–Al2O3 and Mordenite," *Procedia Eng.*, vol. 152, pp. 735–741, 2016.

[98] G. M. Dhar, B. . Srinivas, M. . Rana, M. Kumar, and S. . Maity, "Mixed oxide supported hydrodesulfurization catalysts—a review," *Catal. Today*, vol. 86, no. 1–4, pp. 45–60, Nov. 2003.

[99] V. K. Gupta, I. Ali, T. A. Saleh, M. N. Siddiqui, and S. Agarwal, "Chromium removal from water by activated carbon developed from waste rubber tires," *Environ. Sci. Pollut. Res.*, vol. 20, no. 3, pp. 1261–1268, 2013.

[100] C. Liang, Z. Li, and S. Dai, "Mesoporous carbon materials: synthesis and modification.," *Angew. Chem. Int. Ed. Engl.*, vol. 47, no. 20, pp. 3696–717, 2008.

[101] C. Fontaine, Y. Romero, A. Daudin, E. Devers, C. Bouchy, and S. Brunet, "Insight into sulphur compounds and promoter effects on Molybdenum-based catalysts for selective HDS of FCC gasoline," *Appl. Catal. A Gen.*, vol. 388, no. 1–2, pp. 188–195, 2010.

[102] A. Tougerti, E. Berrier, A. S. Mamede, C. La Fontaine, V. Briois, Y. Joly, E. Payen, J. F. Paul, and S. Cristol, "Synergy between XANES Spectroscopy and DFT to Elucidate the Amorphous Structure of Heterogeneous Catalysts: TiO2-Supported Molybdenum Oxide Catalysts," *Angew. Chemie - Int. Ed.*, vol. 52, no. 25, pp. 6440–6444, 2013.

[103] T. Bhaskar, K. R. Reddy, C. P. Kumar, M. R. V. S. Murthy, and K. V. R. Chary, "Characterization and reactivity of molybdenum oxide catalysts supported on

zirconia," *Appl. Catal. A Gen.*, vol. 211, no. 2, pp. 189–201, 2001.

[104] L. J. Konwar, P. Mäki-Arvela, E. Salminen, N. Kumar, A. J. Thakur, J. P. Mikkola, and D. Deka, "Towards carbon efficient biorefining: Multifunctional mesoporous solid acids obtained from biodiesel production wastes for biomass conversion," *Appl. Catal. B Environ.*, vol. 176–177, pp. 20–35, 2015.

[105] S. Kang, J. Ye, and J. Chang, "Recent Advances in Carbon-Based Sulfonated Catalyst:\rPreparation and Application," *Int. Rev. Chem. Eng.*, vol. 5, no. 2, pp. 133–144, 2013.

[106] X. Y. Liu, M. Huang, H. L. Ma, Z. Q. Zhang, J. M. Gao, Y. L. Zhu, X. J. Han, and X. Y. Guo, "Preparation of a carbon-based solid acid catalyst by sulfonating activated carbon in a chemical reduction process," *Molecules*, vol. 15, no. 10, pp. 7188–7196, 2010.

[107] A. Omri and M. Benzina, "Influence of the origin of carbon support on the structure and properties of TiO2 nanoparticles prepared by dip coating method," *Arab. J. Chem.*, 2015.

[108] H. Farag, I. Mochida, and K. Sakanishi, "Fundamental comparison studies on hydrodesulfurization of dibenzothiophenes over CoMo-based carbon and alumina catalysts," *Appl. Catal. A Gen.*, vol. 194–195, pp. 147–157, Mar. 2000.

[109] M. Kouzu, Y. Kuriki, F. Hamdy, K. Sakanishi, Y. Sugimoto, and I. Saito, "Catalytic potential of carbon-supported NiMo-sulfide for ultra-deep hydrodesulfurization of diesel fuel," *Appl. Catal. A Gen.*, vol. 265, no. 1, pp. 61–67, 2004.

[110] N. Escalona, J. Ojeda, J. M. Palacios, M. Yates, J. L. G. Fierro, A. L. Agudo, and F. J. Gil-Llambías, "Promotion of Re/Al2O3 and Re/C catalysts by Ni sulfide in the HDS and HDN of gas oil: Effects of Ni loading and support," *Appl. Catal. A Gen.*, vol. 319, pp. 218–229, 2007.

[111] H. Farag, D. D. Whitehurst, K. Sakanishi, and I. Mochida, "Carbon versus Alumina as a Support for Co-Mo Catalysts Reactivity towards HDS of Dibenzothiophenes and Diesel Fuel," *Catal. Today*, vol. 50, no. 1, pp. 9–17, 1999.

[112] P. Gheek, S. Suppan, J. Trawczyński, A. Hynaux, C. Sayag, and G. Djega-Mariadssou, "Carbon black composites-supports of HDS catalysts," *Catal. Today*, vol. 119, no. 1–4, pp. 19–22, 2007.

[113] J. Chen, H. Yang, and Z. Ring, "HDS kinetics study of dibenzothiophenic compounds in LCO," in *Catalysis Today*, 2004, vol. 98, no. 1–2 SPEC. ISS., pp. 227–233.

[114] S. A. Ganiyu, K. Alhooshani, and S. A. Ali, "Single-pot synthesis of Ti-SBA-15-NiMo hydrodesulfurization catalysts: Role of calcination temperature on dispersion and activity," *Appl. Catal. B Environ.*, vol. 203, pp. 428–441, 2017.

Vitae

Name	:Umar Cheche Abubakar
Nationality	:Nigerian
Date of Birth	:9/25/1987
Email	:abubakarcheche@gmail.com
Address	10B Kaduna road, Dutsen Kura, Minna, Niger State.

ACADEMIC BACKGROUND

MSc Chemistry:	King Fahd University of Petroleum and Minerals, Dhahran, Kingdom of Saudi Arabia.	2014-2017
BSc Chemistry:	Usmanu Danfodiyo University, Sokoto, Sokoto State. Nigeria	2006-2010

EXPERIENCE

Graduate Assistant:	Usmanu Danfodiyo University, Sokoto. Sokoto State, Nigeria.	2013-Date